UNIVERSITY OF CAPE COAST

ASSESSING THE IMPACT OF CLIMATE AND LAND USE LAND COVER CHANGES ON FLOOD RISKS IN THE ANKOBRA RIVER BASIN COASTAL AREA IN GHANA

BY

TCHAKA PULUMUKA KAMANGA

Thesis submitted to the Department of Fisheries and Aquatic Sciences, School of Biological Sciences, University of Cape Coast, in partial fulfilment of the requirements for award of Masters of Philosophy degree in Integrated Coastal Zone Management

OCTOBER 2024

ABSTRACT

Besides ocean processes, coastal flood risk is underlined by climate and land use land cover (LULC) changes and intrinsic socio-economic characteristics of coastal inhabitants. This study assessed the impacts of temperature, rainfall and LULC changes on flood risks in the Ankobra River Basin Coastal Area (ACA), in the Western Region of Ghana. Trend analysis using Mann-Kendal trend test (Z_{MK}) was used to assess changes in temperature and rainfall between 1986 and 2021. Maximum Likelihood Classification was used to assess LULC change between 1991 and 2022. Socio-economic data were collected through household interviews comprised of 341 households. A Frequency analysis of socio-economic factors was performed in SPSS, followed by variable weighting using Analytical Hierarchy Process (AHP), development of vulnerability indices using the Square Root of Mean of Product formula and hydrological modelling using the Soil and Water Assessment Tool (SWAT) model. The study showed a significant increase in temperature (Z_{MK} = 3.392). Also, the study found that the basin is dominated by dense vegetation (DV), cultivated/sparse vegetation (CV), built-up/bare land (BL) and water (WT). In all, DV decreased by 46 % at the expense of increase in land covered by CV, BL and WT. These changes had corresponding water yield of 335.64 mm in 1991, resulting in inundation area of 14.89 km^2, 494.91 mm in 2008 resulting in inundation area of 23.50 km^2 and 481.91 mm in 2021resulting in inundation area of 18.31 km^2. The vulnerability of the ACA is principally driven by elevation, distance to coastline, condition of houses and income levels.

KEY WORDS

Coastal vulnerability

Climate change

Flood risk

Land use land cover

Vulnerability index

SWAT Model

ACKNOWLEDGEMENTS

I am profoundly thankful to my supervisors, Dr. Noble Kwame Asare and Dr. Donatus Bapentire Angnuureng, both of the Department of Fisheries and Aquatic Sciences (DFAS) of the University of Cape Coast (UCC), for supervising this research work, Mr Richard Adade of Centre for Coastal Management (CCM), and Dr. Ebenezer Boateng of Department of Geography, UCC, for their technical assistance in GIS applications, without whom the work would have stalled.

I am also thankful to the World Bank and the Government of Ghana for making available financial support through the Africa Centre of Excellence in Coastal Resilience (ACECoR) project, from which this work got funding. Along the same, I am indebted to the leadership and management of CCM and the DFAS of UCC, for overall administrative support in the course of this work.

Lastly but not the least, my acknowledgement goes to the people of Nzema East and Ellembelle Districts in Ghana, who participated in the survey, and the field assistants who assisted me in data collection, and fellow students, particularly, Dr. Lukhabi, who took time to read through the work, and made significant editorial input to it.

DEDICATION

To Mwattipa and Abrianna, and in memory of my Grandfather, Mr. MacLean Nkosi.

TABLE OF CONTENTS

	Page
DECLARATION	ii
ABSTRACT	iii
KEY WORDS	iv
ACKNOWLEDGEMENTS	v
DEDICATION	vi
TABLE OF CONTENTS	vii
LIST OF TABLES	xi
LIST OF FIGURES	xiii
LIST OF ACRONYMS	xv
CHAPTER ONE: INTRODUCTION	
1.1 Background to the Study	1
1.2 Statement of the Problem	3
1.3 Purpose of the Study	5
1.4 Research Aim and Objectives	5
1.5 Hypothesis	5
1.6 Research Questions	6
1.7 Significance of the Study	6
1.8 Delimitations	6
1.9 Limitations	7
1.10 Definition of Terms	7
1.11 Organisation of the Study	8
CHAPTER TWO: LITERATURE REVIEW	
2.1 Floods: Causes, impacts and trend	10

2.2 Types of floods 12

2.3 Hydrological cycle and flooding 15

2.4 Floods in Ghana 17

2.5 The concept of disaster risk in relation to floods 19

2.6 LULC and flood risk 21

2.7 Climate change and flood hazard 22

2.8 Vulnerability Assessment 25

2.8.1 Principal Component Analysis 29

2.8.2 Analytical Hierarchical Process 30

2.9 Physical and socio-economic determinants of coastal vulnerability 32

CHAPTER THREE: MATERIALS AND METHODS

3.1 Research design 34

3.2 Study Area 34

3.3 Data Acquisition 36

3.1.1 Satellite data 37

3.1.2 Temperature and Rainfall Data 38

3.1.3 Socio-economic Data 39

3.1.3.1 Sampling procedures 40

3.1.3.2 Data collection instruments 40

3.1.4 Soil and Water Assessment Tool (SWAT) Model Data 41

3.4 Data Preparation 43

3.4.1 Satellite Data 43

3.4.2 Temperature and Rainfall data 43

3.4.3 Socio-economic data 44

3.4.4 SWAT Model data 46

3.4.4.1 Preparation of Digital Elevation Model (DEM) data 46

3.4.4.2 Preparation of land use data 47

3.4.4.3 Preparation of soil data 49

3.4.4.4 Preparation of weather data 50

3.5 Data Analysis 51

3.5.1 Land use land cover change analysis 51

3.5.1.1 Land cover classification 51

3.5.1.2 Accuracy assessment and change detection 51

3.5.1.3 Temperature and rainfall change analysis 52

3.5.1.4 Vulnerability analysis 53

3.5.2 Hydrological modelling and flood mapping 54

3.5.2.1 Watershed delineation 54

3.5.2.2 Hydrological Research Unit (HRU) analysis 54

3.5.2.3 Weather data input 55

3.5.2.4 Calibration, validation and model performance evaluation 55

3.5.2.5 Mapping of flood risk in the Ankobra Coastal Area 56

CHAPTER FOUR: RESULTS

4.1 LULC Changes in the ARB between 1991 and 2022. 57

4.1.1 Land use land cover change 57

4.1.2 Land use land cover transition 61

4.2 Climate variability in the ARB between 1991 and 2021 62

4.3 Vulnerability of the Coastal Area in the ARB to Flooding 66

4.3.1 Socioeconomic and physical characteristics of ACA 66

4.3.2 Weighting of vulnerability variables 70

4.3.3 Vulnerability indices 72

4.3.4 Vulnerability mapping 73

4.4 Extent of flooding due to climatic changes in the ACA 76

4.4.1 Watershed delineation and Hydrological Response Unit (HRU) analysis 76

4.4.2 SWAT Calibration, validation and performance evaluation 77

4.4.3 Water yield generation 79

4.4.4 Correlation between water yield and land use and climatic factors in ARB 80

4.4.5 Mapping of flood inundation in the ACA 82

CHAPTER FIVE: DISCUSSIONS

5.1 Introduction 85

5.2 Land use land cover change in the Ankobra River Basin 85

5.3 Temperature and rainfall variations in Ankobra river basin 86

5.4 Impacts of variations in LULC, rainfall and temperature on water yield in Ankobra River Basin 88

5.5 Coastal Vulnerability and Flood Risk in the ACA due to Climate and LULC Changes in the ARB 89

5.5.1 Socio-economic and physical determinants of vulnerability in ACA 89

5.5.2 Water yield and flood risk in the ACA 92

CHAPTER SIX: CONCLUSIONS AND RECOMMENDATIONS 95

REFERENCES 98

APPENDICES 118

LIST OF TABLES

Table		Page
1	Values for the random index (RI) for particular number of criteria (N)	32
2	Common variables that determine coastal vulnerability	33
3	Characteristics of satellite images used in the study	38
4	Particulars of climate data for the basin	39
5	Particulars of the Meteorological stations	42
6	Ranking of socio-economic variables for determining vulnerability	45
7	Ranking of physical variables for determining vulnerability	46
8	Land use look-up table for SWAT input	48
9	Soil use look-up table for SWAT input	50
10	Land Use Classification Scheme Adopted from FAO Land Classification System	52
11	Land Use change in Ankobra Basin between 1991 and 2022	60
12	Temperature Change in the Ankobra Basin between 2000 and 2013 for Benso Station and 1986 to 2020 for Sefwi-Bekwai Station	63
13	Rainfall Change in Ankobra Basin, calculated based on linear trend line	65
14	Frequency (in %) of socio-economic variables in ACA, and their ranking	69
15	Magnitude of physical variables in ACA and their ranking	70
16	Weight of socio-economic and physical variables in influencing coastal vulnerability in ACA	71
17	Vulnerability Indices for the studied communities in the ACA	72

18	Level of Vulnerability for coastal communities based on social and physical factors	74
19	Soil and slope characteristics in the ARB	77
20	SWAT model performance evaluation statistics	79
21	Estimated water yield from the ARB	79
22	Variations in land use and hydro-climatic parameters	81
23	Correlation among hydro-climatic parameters in the ARB	82
24	Estimated inundated coastal area due to climate and LULC change in the ARB	83

LIST OF FIGURES

Figure		Page
1	Flood event between 1998 and 2008.	11
2	Map of study area showing the Ankobra Rier Basin (Above) and the Ankobra Coastal Area (Below)	36
3	Digital Elevation Model (DEM) data extracted for SWAT input	47
4	Land use map for the Ankobra River Basin prepared for SWAT input	49
5	LULC maps for Ankobra Basin in 1991 (A), 2008 (B), 2016 (C) and 2022 (D)	59
6	Land use transition for ARB between 1991 and 2022	61
7	Temperature trend at Benso Meteorological station	62
8	Temperature trend at Sefwi-Bekwai Meteorological station	63
9	Monthly Mann-Kendall trend test for temperature at Benso and Sefwi-Bekwai Stations	63
10	Rainfall trend at Benso weather station	64
11	Rainfall trend at Sefwi Bekwai Meteorological Station	65
12	Monthly Mann-Kendall Trend test for Rainfall at Benso and Sefwi-Bekwai Stations	66
13	Index-based social (A), physical (B) and integrated (C) vulnerability maps of ACA	75
14	SWAT outputs for the ARB- Sub-basins (A) and Soil types (B)	77
15	SWAT Model Calibration for the ARB	78
16	SWAT Model Validation for the ARB	78

17 Coastal flood risk map due to climate and LULC change in the Ankobra River Basin 84

LIST OF ACRONYMS

ACA	Ankobra Coastal Area
ACF	Autocorrelation coefficient function
AHP	Analytical Hierarchy Process
ARB	Ankobra River Basin
ACA	Ankobra River Basin Coastal Area
ASTER-V3	Advanced Spaceborne Thermal Emission and Reflection Radiometer Version 3
CI	Consistency Index
CoG	Cost of Ghana
CR	Consistency Ration
DEM	Digital Elevation Model
DFO	Dartmouth Flood Observatory
DSMW	Digitised Soil Map of the World
ACECoR	Africa Centre of Excellence in Coastal Resilience
ETM	Enhanced Thematic Mapper
FAO	Food and Agriculture Organisation
GIS	Geographical Information System
GMET	Ghana Meteorological Agency
HRU	Hydrological Response Unit
LULC	Land use land cover
MLC	Maximum Likelihood Classification
NASA	National Aeronautics and Space Administration
NSE	Nash-Sutchiffe coefficient
PBIAS	Performance bias

PCA	Principal Component Analysis
PCM	Pairwise Comparison Matrix
PVI	Physical Vulnerability Index
SPSS	Statistical Package for Social Science
SST	Sea surface temperature
SVI	Social Vulnerability Index
SWAT	Soil and Water Assessment Tool
TM	Thematic Mapper
TM+	Thematic Mapper Plus
UNESCO	United Nations Educational, Scientific and Cultural Organisation
USGS	United States Geological Survey
WGEN	Weather Generator
Z_{MK}	Mann-Kendal trend test

CHAPTER ONE

INTRODUCTION

1.1 Background to the Study

Globally, floods are among the most significant natural calamities that affect many regions of the world (Demir & Kisi, 2016). In the 1990s, few historical floods were reported with the 1991 and 1994 Bangladesh events being historical (Loster, 1999). Thereafter, more events with increased frequency and associated damage were recorded, indicating an increasing trend. Globally, 2900 flood incidents were documented between 1998 and 2008. Generally, floods occur in every country with the exception of those that are located at latitudes higher than 60° that are more susceptible to flooding (Adhikari, Hong, Douglas, Kirschbaum, Gourley, Adler, and Brakenridge, 2010)). According to Zou, Lele & Thomalla (2008), floods were the highest reported disasters from 1993 to 2006, accounting for 47.6 % of fatal global natural disasters and 16.7 % of deaths from natural disasters. Also, flooding accounted for the largest proportion of economic loss, estimated at about US$300 billion

The impact associated with a flood disaster is dependent on the factors that are principal to its generation, as well as area of impact. Based on this, coastal floods are the most damaging type of floods. Two main factors contribute to this. Firstly, coastal areas are generally low-lying areas and more exposed to oceanic processes such as Sea Level Rise (SLR) (Bengal, Bhattacharya, & Guleria, 2012) With the increasing climate change impacts on sea level, coastal areas are most affected, and the situation is projected to worsen (Sagoe-Addy & Appeaning-Addo (2013). Secondly, coastal areas are

among the most populated areas of the world (Hinkel, Lincke, Vafeidis, Perrette, Nicholls, Tol, Marzeion, Fettweis, Ionescu, & Levermann, 2014). Over two-thirds of the world's population is located within coastal areas, with a myriad of socio-economic assets such as homes, schools, hospitals, factories and businesses (Arnous & Green, 2011). A single flood event in coastal areas is therefore most likely to do unprecedented harm.

According to Najibi and Devineni (2018), the situation is worse in the tropical areas, where flood frequency and duration is the highest. In the Gulf of Guinea and the Coast of Ghana (CoG), floods are already being experienced with increased frequency and severity, and are predicted to worsen under future socio-economic and climatic conditions (Evadzi, Zorita and Hünicke, 2017).

Aside sea-level rise resulting from global warming, Dasgupta and Meisner (2009) and Mimura (2013) attest to the significance of local factors at the coastal level in contributing to the increasing probability of flooding in coastal areas. Anthropogenic land uses, which affect land cover and hydrological response in the coastal areas, and other LULC changes in watersheds directly affect the volume of runoff produced by a particular event of (Brath, Montanari, & Moretti, 2006; Hussein, Alkaabi, Ghebreyesus, Liaqat & Sharif, 2020; Saghafian, Farazjoo, Bozorgy & Yazdandoost, 2008; Sheng & Wilson, 2009). Sharif, Al-Juaidi, Al-Othman, Al-Dousary, Fadda, Jamal-Uddeen and Elhassan (2016) found an increase in peak discharge by about 30% following a 15% increase in urbanisation in Al-Aysen, Riyadh. However, these occurrences have been less considered in coastal flood risk studies in the

Gulf of Guinea, and particularly, along the CoG, where the focus has been mainly on impact of SLR on coastal vulnerability (Evadzi et al., 2017).

Flood risk is defined with regards to impacts and responses of the systems at risk (Bagewadi, 2017; Kang, Oh, Lee, & Jeong, 2018; Reisinger, Howden, Vera, Garschagen, Hurlbert,.2020). It is therefore dependent on the characteristics surrounding the flood as a hazard on one hand, and coastal vulnerability on the other. The characteristics therefore define the sensitivity of the adaptive capacity of the system at risk and its exposure to the impacts of the flood event (Dolan & Walker, 2006; Phongsapan, Chishtie, Poortinga, Bhandari, Meechaiya, 2019). These factors are either physical, socio-economic or both (Ahsan & Warner, 2014; Aman, Tano, Toualy, Silué, Addo, & Folorunsho, 2019; Boateng, Wiafe, & Jayson-Quashigah, 2016; Cutter, Boruff, & Shirley, 2003; Fekete, 2009; Ge, Dou, & Liu, 2017; Hadipour, Vafaie, & Deilami, 2020; Maanan, Rueff, Adouk, Zourarah, & Rhinane, 2018; Rocha, Antunes, & Catita, 2020). Despite the importance of socio-economic factors in defining coastal vulnerability, and flood risks, vulnerability studies along the CoG and the Gulf of Guinea, (e.g. Aman et al., 2019; Boateng et al., 2016) focused more on physical factors, and less on socio-economic factors. This current study therefore has the potential of leading to designing appropriate strategies for managing flood risks in the CoG.

1.2 Statement of the Problem

There is evidence (e.g. Berihun, Tsunekawa, Haregeweyn, Meshesha, D. Adgo, 2019; Jevrejeva, Palanisamy, & Jackson, 2020; Lyu, Zhang, & Church, 2020) that flooding from global sea-level rise (SLR) due to global climate change, is threatening the CoG. However, localised climatic and non-climatic

factors, mainly anthropogenic land use activities, play a significant role in relative SLR and coastal flooding (Berihun et al., 2019; 2020; Lyu et al., 2020; Mimura, 2013). Despite this, there is a knowledge gap regarding empirical evidence on the impact of localised climate and LULC variations on coastal flood risk in Ghana.

Secondly, hazard characteristics and the vulnerability of the elements at risk determine disaster risk. In the context of coastal flood, physical and socio-economic factors are key (Aman et al., 2019; Boaten et al., 2016; Fekete, 2009; Hadipour et al., 2020; Kang et al., 2018; Marzi, Mysiak, Essenfelder, , Amadio, Giove, & Fekete, 2019), and apply to the coast of Ghana (CoG). The factors need to be determined to comprehensively understand coastal flood disaster risk. Despite this, vulnerability assessments along the CoG have mainly focused on geological or physical factors with less regard to the impacts of socio-economic factors (Boateng et al., 2016, Evadzi et al., 2017; Aman et al., 2019). There is, therefore, a knowledge deficit in the impacts of combined physical and socio-economic characteristics on the vulnerability of coastal communities, which this research intends to contribute to addressing, with a special focus on the western CoG.

Lastly, estimation of present and future flood risks along the CoG is less comprehensive because it is mainly based on oceanic processes, and disregards the contribution of land-based processes that have impact on water yield, particularly LULC in the adjacent basins. This situation has the potential to influence appropriate adaptation actions in coastal areas.

1.3 Purpose of the Study

The general purpose of this study was to impacts of climate and land use/land cover change in Ankobra River Basin on coastal flood risk in the Ankobra Coastal Area in the Western Region of Ghana.

1.4 Research Aim and Objectives

The overall aim of this study was to assess the impacts of climate and land use/land cover change in ARB on coastal flood risk in the ACA in the Western Region of Ghana.

The specific objectives of this study were to;

1. Determine land use and land cover changes in the ARB between 1991 and 2021.
2. Assess climate variability in ARB using temperature and rainfall data between 1991 and 2021.
3. Assess vulnerability of the ACA to coastal flooding based on physical and socio-economic factors.
4. Estimate the extent of coastal flooding in ACA based on the measured climate and LULC changes in the ARB.

1.5 Hypothesis

The study had the following hypotheses in line with the objectives of the study, the following were the hypotheses:

There were no significant variations in temperature and rainfall in the Ankobra River Basin between 1991 and 2021.

The changes in land cover, temperature and rainfall in the Ankobra River Basin did not have significant impact on water yield, and hence, flood risk in the Ankobra Coastal Area between 1991 and 2021.

1.6 Research Questions

1. What are the principal physical and social determinants of vulnerability of Ankobra Coastal Area to coastal flooding?

1.7 Significance of the Study

Assessing the impacts of climate and land use/land cover change on coastal flood risk in the Ankobra Coastal Area (ACA) in Ghana will provide information for integrating present and future coastal zone flood risk management, specifically through the provision of risk information for appropriate response. This thesis additionally contributes to the attainment of Sustainable Development Goals (SDGs) number 11-"Sustainable Cities and Communities" and 13- "Climate Action", the overall objectives of the Sendai Framework for Disaster Risk Reduction (UNISDR, 2015) and Agenda 2063 (African Union Commission, 2015). Further, the findings of the thesis could be used to help in formulation of adaptation strategies for the coastal areas, therefore contributing to building coastal resilience in line with Act 927/2016 of the Government of Ghana.

1.8 Delimitations

Among many other parameters that are used to define climate, and hence climate change, this study only used temperature and rainfall. This was because temperature and rainfall were the most consistently recorded parameters by the Ghana Meteorological Agency for the meteorological stations located in the ARB and were therefore readily available. Temperature and rainfall are also the widely sued parameters used for measuring, for example, they have been mostly used by the IPCC in the production of climate change assessment reports (ARs) (Zhou, 2021).

Also, there are many determining factors of vulnerability of coastal areas to flooding. This study however considered only wave height, tide range, elevation and distance as determinants of physical vulnerability. For social vulnerability, the study considered only population, age, sex, employment, education, cohesion among community members and access to productive natural resources. Data collect against these variables only focused on household heads. The choice of these physical and socio-economic parameter was informed by extensive literature review.

The study focused on a period between 1991 and 2021, the focus on changes in climate parameters and land use/land cover in the Ankobra River Basin, and their impacts on disaster risk on the coastal communities situated in the coastal area of the Basin.

1.9 Limitations

To assess land use land cover change, the study used free Landsat satellite images that were acquired from open sources due to costs implications. The spatial resolution of the free sourced images was limited to only 30 metres. The low spatial resolution contributed to Kappa values of less than 1 during accuracy assessment of land use classification. The coastal areas also usually have high cloud cover, as such it was difficult to acquire satellite images with less cloud cover at a fixed interval for consistent comparison among assessment periods.

1.10 Definition of Terms

Vulnerability: The conditions determined by physical, social, economic and environmental factors or processes which increase the

susceptibility of an individual, a community, assets or systems to the impacts of hazard

Climate change

Flood Risk: The potential loss of life, injury, or damaged which could occur to a system, society or a community in a specific period of time, determined probabilistically as a function of exposure and vulnerability to floods.

Land use: Utilisation of the land by human for different objectives, addressing different needs.

Land cover: The biophysical state of the earth surface and subsurface.

Vulnerability index: A measure of the exposure of an element to some hazard expressed as a composite of multiple quantitative indicators that deliver a single numerical result.

1.11 Organisation of the Study

The study is organised in 5 chapters aside the perquisites sections. Chapter One is the introduction of the study. It provides a background to the study which describes the context in which the problem that motivated the study occurs. In line with the background, the statement of the problem is highlighted which points out existing knowledge gap, based on this, the purpose of the study along with the main objectives, specific objectives, hypotheses and research questions are presented. The chapter also outlines the significance of the study which points how the results of the study would be used; delimitations which defines the scope of the study as well as limitations of the study. The chapter also provides definitions of the key terms.

Chapter Two is the literature review and outlines the conceptual framework that underpins the study. It outlines key concepts and theories around which the study is built.

Chapter Three of the study is the research methods. It describes the research design that was employed in the study, the study area, types of data used, the target population, sampling methods, data collection procedures, and the analyses that were undertaken.

Chapter Four of the study presents the results of the study in line with the four research objectives that aimed at assessing the flood risk in the ACA based on the impacts of climate and LULC changes in the ARB.

Chapter Five discusses the results by examining the implications with resect the theoretical position of the study. It also interprets the findings in reference to relevant literature and past findings

Chapter Six of the study outlines the conclusion and recommendation regarding the study. It provides an overview of the entire study and outlines recommendations based on the key findings of the study. It also provides suggestions for further research.

The last section of the organisation of the work lists all the work that was reviewed and cited regarding the study.

CHAPTER TWO

LITERATURE REVIEW

2.1 Floods: Causes, impacts and trend

Globally, floods are one of the most common significant natural calamities affecting many regions of the world (Demir & Kisi, 2016). In the 1990s, few historical floods were reported, with 1991 and 1994 Bangladesh events being the most impactful (Loster, 1999). Over the years, more events with increased frequency and associated damage were recorded, indicating an increasing trend as noted by Abass, Dumedah, Frempong, Muntaka, Appiah, Garsonu and Gyasi (2022). For example, between 1998 and 2008, Adhikari et al. (2010) reported that a total of 2900 flood events were recorded globally with practically every country, with the exception of those that are located at latitudes higher than 60° being susceptible to flooding (Figure 1). According to Zou, Lele & Thomalla (2008), floods were reported between 1993 and 2006 as the second most fatal global natural disasters accounting for 16.7% of deaths from natural disasters. Floods were also responsible for the highest economic damage among natural disasters, causing over 26% of the total estimated global damage of US$1.1 trillion.

According to Adhikari et al. (2010), 247,000 fatalities were registered between 1998 and 2008, averaging 22,500 deaths per year. Despite the United States of America having registered the most flood events, damage was however high in Asia, Africa and Central America.

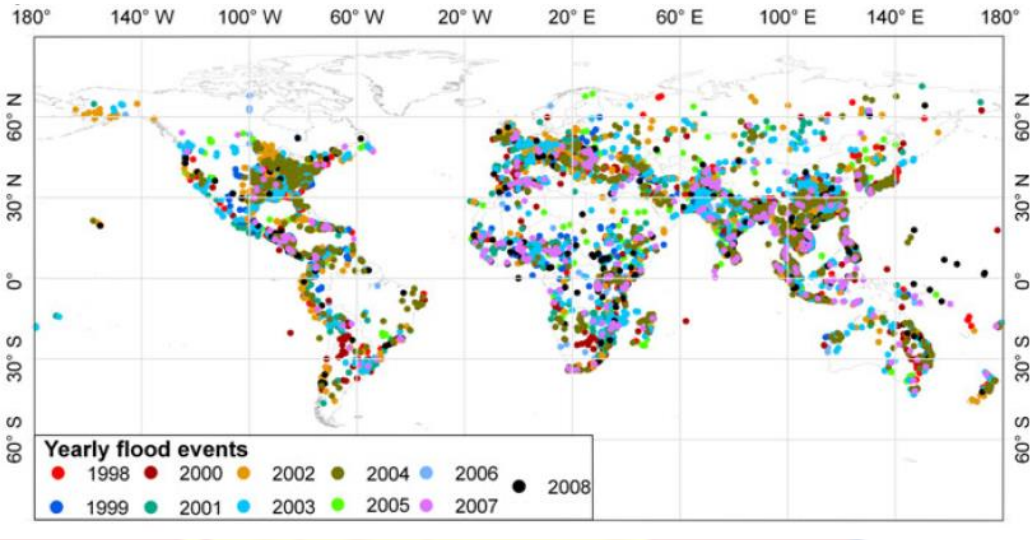

Figure 1: Flood event between 1998 and 2008.
Source: Adhikari et al., 2010

Some studies, for example, Tanoue, Hirabayashi, & Ikeuchi (2016) attribute the global increasing trend of flood cases to improved reporting about the flood events, and not the actual increase in flood occurrences. While improved reporting helps availing data necessary for establishing flood trends, evidence on the actual increase in the flood occurrence is however enormous. For example, Najibi & Devineni (2018) explored flood trends using Dartmouth Flood Observatory (DFO) data from 1985 to 2015 and confirmed the increasing number of flood events and severity. Further to this, Adhikari et al. (2010) found an association between climate change and flood occurrence. Increasing extreme climatic events, such as heavy rainfall cyclones resulted in increased global occurrence of flood events between 1998 and 2008.

The increasing flood events, both in occurrence and magnitude, are associated with climate change and changes in land use and land cover (Berihun et al., 2019; Pour, Khairi, Wahab, Shahid & Dewan, 2020) . Confirming this, Xuan Do et al. (2020) found a significantly high level of change in floods under the Intergovernmental Panel on Climate Change

(IPCC) Representative Concertation Path (RCP) 2.6 and RCP6.0 future climate change scenarios in individual regions. Also, Nka, Oudin, Karambiri, Paturel & Ribstein (2015) found an increasing trend in frequency and magnitude of floods in all catchment areas in West Africa, except the Sudanian catchment area, as a result of climate induced rainfall extremes and catchment degradation.

The impacts of land use and land cover change as antecedent conditions which modify the runoff response are confirmed by various studies, for example, Dasgupta and Meisner (2009), Wasko (2021) and Mimura (2013). According to Schulze (2000) land use refers to the utilisation of the land by humans, to achieve different objectives and for addressing different needs. Also, it includes effective management and is subject change by social, political and economic forces. Further, Brath, Montanari & Moretti (2006), Hussein et al. (2020), Saghafian et al. (2008) and Sheng & Wilson (2009) posited that LULC change in a particular basin directly affects the volume of runoff from a given event of rainfall, hence flooding. This assertion is supported by Baldassarre et al. (2010) and Abass et al. (2022) who found out that, in Africa and in Ghana increase in flood events were greatly due to the impacts of urbanization.

2.2 Types of floods

For a flood to be worthy of attention, it must be associated with impacts or have the potential to cause damage (Reisinger et al, 2020). Otherwise, it will be just a natural phenomenon. The impact associated with a flood is dependent on the factors that are principal to the generation of the floods, as well as the area of impact (Mondal, Murayama & Nishikizawa, 2021). The review of

available literature identified the following flood types; flash floods (Marchi et al., 2010), urban or pluvial floods (Pour et al., 2020), river or fluvial flooding (Prastica & Fanani, 2021) and coastal flooding (Haigh, & Nicholls, 2017). According to Marchi, Borga, Preciso & Gaume (2010) localized heavy downpours are a common trigger for flash floods. Flash floods typically affect basins of area less than 1000 km^2. The response time for flash floods is usually few hours. Different processes and factors affect their generation. These include intense rainfall intensity, soil characteristics such as moisture and hydraulic properties. The generation processes of flash floods are also enhanced by land use changes, for example urbanisation and loss of vegetation cover. According to Gaume, Bain, Bernardara, Newinger, Barbuc (2009), flash flooding is top ranking on the global list of hydrological disasters causing unprecedented number of individual deaths and property destruction.

As the name suggests, urban flooding is termed after the area of impact as well as the underlying factors associated with its generation. According to Pour et al. (2020), impacts of urbanisation on runoff and drainage are key attributes of the generation and impact of urban floods. Urbanisation is associated with reduced natural vegetation cover, and increased extent of impervious areas. These, significantly increase surface runoff at the expense of infiltration. In addition to this, urbanisation is also associated with poorly designed drainage systems that do not take into account future scenarios, which make them all conducive for urban flooding (Abass et al., 2022). With increased climate induced rainfall intensities, urban areas more often become inundated and suffer urban flooding. This provides clear evidence about the combined effects that the interaction of land use and climate change on hydro-

hazards. As a result of this interaction, many cities in the world have suffered property losses (Liu & Niyogi, 2019), with Ghana being no exception. Risk analysis of urban flooding by Abass et al. (2022), however, shows the importance of anthropogenic factors, such as unregulated urbanisation, insufficient drainage structure, lack of effective means for solid waste management, and inadequate regulatory and institutional framework on urban flooding in Ghana.

River flooding is another type of flooding, and is characterised by longer duration, and generated from a relatively larger basin than that of flash flooding. According to Syvitski & Robert Brakenridge (2013), river flooding is incited by a prolonged heavy rainfall in basins, which leads to peak flows than can be contained by a river confinement, or where levees of a river fail leading to inundation of the nearby areas. Elsewhere, change in land cover has been linked to increased dynamics of discharge return period leading to the inability of a river to accommodate flooding volume (Prastica & Fanani, 2021).

Coastal flooding has become almost synonymous to SLR due to the weight that is given to climate change induced SLR. However, according to Vitousek, Barnard, Fletcher, Frazer, Erikson, & Storlazzi (2017) , SLR that occur in most coastal areas is significantly smaller than normal ocean-level variations caused by ocean processes such as storm surge waves, and tides. This implies that, the uniqueness of coastal flooding is multifaceted unlike the other types of flooding. It is caused by various ocean processes like storm surge waves and tides whose impact has been exacerbated by climate induced SLR (Katsman et al., 2008)

Aside global warming induced SLR, local factors at the coast significantly contribute to increasing the likelihood of coastal flooding. Principally, anthropogenic land uses affect land cover and hydrological response in coastal areas (Dasgupta & Meisner, 2009 and Mimura, 2013). LULC change in a watershed directly affects the volume of runoff produced from a particular rainfall event (Brath et al., 2006; Hussein et al., 2020; Saghafian et al., 2008; Sheng & Wilson, 2009). Practically, the available literature that the study reviewed does not provide comprehensive information about the socio-economic impacts of coastal flooding emanating from terrestrial surface runoff, mainly because of its local and less extensive nature. In contrast, the impacts of climate induced SLR on coastal flooding have been extensively studied. For example, it has been documented that SRL induced annual flooding is predicted to affect 0.2% to 4.6% of the world's population in the twenty-first century if no adaptation and mitigation actions are taken (Hinkel et al., 2014) . This will lead to annual losses in global gross domestic product of 0.3–9.3%.

It is clear, therefore, that climatic parameters, such as temperature and rainfall, and anthropogenic land use activities, which lead to modification of land cover, are key factors to flood generation. The interaction of the factors and the role in flood generation is well understood though the concept of hydrological cycle.

2.3 Hydrological cycle and flooding

In its summarised version, a hydrological cycle can be described as interrelation of runoff, evapotranspiration, and elements for water storage (Haigh& Nicholls, 2017). The interrelation affects water resource systems

(Yang, Wang, Xia, Chen, Zhan, 2022), hence water availability or scarcity. The cycle is sensitive to changes in both climatic land-based parameters and processes (Kenea, Adeba, Regasa & Nones, 2021). This makes the water resources system inherently sensitive to climate and land use changes. The impacts of temperature and rainfall on the hydrological cycle are typically used to measure the consequences of climate change on water resources systems. (Huntington, 2006). For example, in West Africa, Nka et al. (2015) found a significant association between flood and annual rainfall maxima in 11 watersheds, while Wasko (2021) observed the supremacy of temperature-based models in predicting flood extremes with global warming.

The effects of land processes, on the other hand, are usually seen from the impacts of LULC change (Wang et al., 2009), which alter the dynamics of hydrological elements on land. Confirming this, studies have shown that changes in the land surface characteristics, such as soil properties, surface roughness and vegetation properties, change the terrestrial hydrological system (Angeles, Angeles, & Springs, 2001). For example in a study by Kenea et al. (2021) on the impacts of LULC changes on hydrological processes in the Fincha'a Watershed in Ethiopia showed an increase in both wet and dry stream flow as a result of conversion of land coverage from forest and grassland to build-up areas. As summed up by Berihun et al. (2019) and Gashaw, Tulu, Argaw, & Worqlul (2018), global warming and land use change are unequivocally key factors that drive water availability and regimes of water bodies, leading to either floods or droughts due to their impacts on hydrological cycle.

It is clear that climatic processes and land use activities and their resultant hydrological responses determine the magnitude and other characteristics of a flood. However, the impacts of floods, are dependent not only on these causative factors but also on exposure and vulnerability of elements at risk. According to Bagewadi (2017), Hadipour et al. (2020) and Kang et al. (2018) , vulnerability is determined by factors that influence the sensitivity or adaptive capacity of the element at risk to the damaging effects of a hazard, such as flood inundation. The vulnerability factors, therefore define the degree to which an element can suffer damage. The interaction of flood inundation with the vulnerability factors of an area define the flood risk (Reisinger et al., 2020).

2.4 Floods in Ghana

Major incidents of flooding in Ghana date back to 1990 (Abass, Dumedah, Frempong, Muntaka, Appiah, Garsonu, & Gyasi, 2022). Karley (2016) provides an account of heavy rainfall that induced storm and caused flooding and claimed lives in most parts of Ghana with Accra being most affected in 1999. According to Karley, torrential rains were responsible for the which left 11 people dead and over 100,000 destitute. Since then, there have been recurring flash floods claiming lives and destroying properties with Accra being an epicentre due to its location, with 50% of its population living in a fluvial flood plain of the Densu River and its tributaries in Ghana (Abass , Ahadzie, Mensah, & Simpeh, 2022; Karley, 2016).

According to Douglas et al. (2008), two major factors drive flooding. These are climate change, which affect rainfall characteristics, especially intensity, and anthropogenic activities that change land cover and water

drainage. A study by Cudjoe & Kwabla Alorvor (2021) in Ada East revealed that climate change induced storm surge is responsible for coastal flooding, while Abass et al. (2022) attributed it to increased urban flood (for example in Kumasi, Accra and other coastal areas). Activities such as soil compaction, removal of vegetation, paving and construction, which are associated with urbanisation, block water pathways and alter land surface. The combination of climate change and urbanisation, therefore, leads to enhanced runoff and higher flood frequency, magnitude and duration.

Due to the general realization of the linkage between climate change and anthropogenic activities on floods in Ghana, most studies have responsively concentrated on understanding the current and future impacts of the factors. For example,- Appeaning-Addo, Larbi, Amisigo & Ofori-Danson (2011) investigated the impacts of climate induced SLR on coastal communities and predicted that by 2100, a total area of 0.80 km^2 would be inundated permanently. With this, about 930 buildings would be at risk of damage and would directly affect over 600,000 people in the Dansoman coastal area along the eastern part of the coast of Accra. In the Volta delta communities, key sources of livelihoods and over 70 houses were destroyed by erosion and coastal flooding between 2005 and 2017 (Appeaning Addo et al., 2011).

Apart from focusing on climate change and ocean processes, Osman, Nyarko, & Mariwah (2016), noted that flood cases reported in Ghana largely focuses on urban areas, justified by the higher economic loss from flood hazards in the urban areas than in the rural set ups. This has led to less reporting of flood cases, impacts and studies in rural areas despite the

devastating impacts on rural set ups due to low coping capacity. Because of this, there is little information about flood cases for rural areas like the ACA.

Further to this, studies on the underlying factors of coastal flood rise have focused on climate induced ocean processes such as SLR, with very little regard to localised changes that take place in the adjacent river basins, despite their importance to coastal flood risks (Mimura, 2013). Despite the indication of the flood risk in the ACA as found out by Osman et al. (2016), the impacts of local changes in climate and LULC have not been adequately studied to inform comprehensive flood risk management in the study area.

2.5 The concept of disaster risk in relation to floods

Historically, the need to respond to different challenges (for instance, natural hazards and their risks) has dictated developmental pathways. The word 'risk' has been widely defined based on the sector of focus. However, a general definition is given by the International Organization for Standardization (ISO) as "effect of uncertainty on objects" (Accastello, Cocuccioni & Teich, 2016). Disaster on the other hand is defined as severe alterations in the normal functioning of a system by any event that has the potential to cause the alteration and the hazard (UN International Strategy for Disaster Risk Reduction [UNISDR], 2009). Flood risk is therefore the uncertainties associated with alterations in the normal functioning of a system, for example a community, due to flood events. According to Reisinger et al. (2020), flood disaster risk is defined with regards to impacts and responses by a particular system. It is, therefore, dependent on the characteristics of a hazard on one hand, and vulnerability on the other hand (Bagewadi, 2017; Kang et al., 2018).

Vulnerability is determined by a set of parameters or variables that define sensitivity and adaptive capacity (Dolan & Walker, 2006). Flood risk assessment therefore involves identification and characterisation of individual parameters that determine vulnerability in reference to hazard and its impacts. For example, in the assessment of flood risk levels in the Ankobra estuary in Ghana, Osman et al. (2016) identified and characterised income, gender, education, number of buildings, height of buildings, foundation levels of the buildings, population size, accessibility to credit and land use in the area, among others, as factors determining physical and social vulnerability in the communities. In the Mediterranean basin, Maanan et al. (2018) classified similar factors into coastal characteristics including coastal elevation and distance to coastline; ocean processes (significant wave height) and socio-economic characteristics covering factors that define the socio-economic profile of the community (income, education and land use).

As a construct of hazard and vulnerability, flood risk has a direct link to factors that affect the hydrological cycle on one hand, and those that influence vulnerability on the other hand. Climate change and LULC change are the most singled out drivers of flooding due to their influence on the hydrological cycle (Berihun et al., 2019; Gashaw et al., 2018; Kenea et al., 2021). In the Chaobai River basin in northern China, Wang et al. (2009) used monthly water balance model and fixing-change method to quantify the effects of climate variations and anthropogenic activities on surface runoffs. They found that climate variation was responsible for about 30% change in surface runoffs while anthropogenic activities contributed about 70% to the runoffs generated from the basin. While the study indicated the supremacy of human activities

on changes in surface runoffs also it highlights the significance of both climate change and LULC change in water balance and flood dynamics. Therefore, both climate change and LULC change must form an integral part of flood risk studies.

2.6 LULC and flood risk

LULC patterns are often linked to changes in the hydrological process at the basin level. It affects the water balance and flooding potential of affected areas. According to Schulze (2000), land use refers to the utilisation of the land by human for different objectives, addressing different needs. It is thus subject to political and socio-economic factors. Land cover on the other hand, is the biophysical state of the surface and subsurface, for example, cropland, settlements and water. Land use change therefore determines the type of land cover in a particular area, which in turn influences land dependent processes including hydrological processes, such as surface runoff and infiltration. It is due to this relationship between LULC and hydrological processes that makes LULC one of the key drivers of flooding and flood risk (Berihun et al., 2019).

Numerous studies have demonstrated the influence of LULC change on flood risk. For example, Berihun et al. (2019) found out that a decrease in cultivated land at the expense of natural vegetation resulted in increased flood risk due to enhanced runoff from the upper blue Nile Basin in Ethiopia. In the same basin, while affirming the increased surface flow due to land cover modification from predominantly natural vegetation to predominantly cultivated and built-up land cover classes, Gashaw et al. (2018) found that the changes resulted in reduced dry season flow, lateral flow, groundwater flow and evapotranspiration. In Bangladesh, Adnan et al. (2020) found out that the

construction of polders in the coastal region of Bangladesh modified flood patterns, thus affirming the effects of LULC changes on flood occurrences.

In the Gulf of Mexico, Brody, Highfield, Blessing, (2015) used statistical linear regression models to segregate the influence of different classes of LULC on losses due to floods. The results of the study showed significant reduction in the losses resulting from protecting some land classes, implying the importance of protecting some types of LULC in reducing floods in affected coastal communities.

LULC influences flooding due to its influence on hydrological outputs such as annual flow, wet and dry seasonal flows, surface runoffs and water yield (Gashaw et al., 2018), and flood potential. Similar studies, for example, Lu, Yan, Zhu, Jin, Liu, & Wu (2020), in Lhasa River Basin, China, found a decrease in base flow, local recharge, quick flow and total water yield as a result of not only vegetation change but also changes in precipitation..

From the review of available literature, it is clear that LULC has a direct influence on flood risk. Assessment of LULC must therefore be integrated with flood risk assessment and the assessment of climatic factors. This is because changes in hydrological processes are not only driven by land cover but also by climatic factors (Lu et al., 2020).

2.7 Climate change and flood hazard

It is now a common knowledge that the world is warning up due to anthropogenic introduction of greenhouse gases (GHGs), mainly carbon dioxide into the atmosphere that could result in climate change. According to Zhou (2021), the 2011-2020 decade was about 1.09°C warmer than the 1850-1900 period. Also, anthropogenic activities were responsible for 1.07°C

warming for the period between 1850 to 1900. Going forward, it is almost certain that the average surface warming will continue to increase, with terrestrial increase being higher than that of the ocean during the 21st century (Gladilshchikova & Semenov, 2017). Variations are however, expected across seasons and regions such that the extent of regions that experience decreasing or increasing inter annual seasonal mean temperatures are expected to increase.

According to IPCC (2021), global variations in temperature have significant corresponding changes in precipitation. Specifically, precipitation will generally increase over high latitudes and in the tropical oceans but it would likely decrease over large parts of the subtropics. Precipitation being an integral element of the hydrological cycle, its sensitivity to global warming affirms the linkage between climate change and flood generation. As noted by Berihun et al. (2019) and Kenea et al. (2021), temperature and rainfall form critical variables to be considered in assessing flood hazard because they dictate the sole input variable of water balance (Daly, Calabrese, Yin, & Porporato, 2019) at basin level, and influence the amount of water yield (Kenea et al., 2021), hence flood.

Due to its significance in determining flood hazard climate and its variable orchange, has taken a central stage in flood risk studies. For example, in South Korea, Park & Lee (2020), investigated the possible future coastal flood risk based on climate change scenarios using machine learning algorithms, and found that flood risk changes based on a particular representative concentration pathway (RCP) climate change scenario, with RCP 8.5 produce a higher risk than RCP 4.5. This shows that in South Korea

(along the South Korean coast) flood risk increases as the temperature rises. Apart from this revelation they also found out that changes in flood risk varies spatially based on the geographical characteristics of affected coast. The southern coast displayed higher risk than the eastern and western coasts for both RCP4.5 and RCP8.5 scenarios. This confirms the influence of spatial variation on the effect of climate change and flood risk as predicted by IPCC (2021) that different regions will respond differently to climate change.

According to Jury & Lucio (2004), localised sea surface temperature (SST) in Mozambique has increased by more than 1°C, pushing it above 28°C as a result of global warming. The increase is beyond the threshold for maintaining deep convection that supports tropical cyclones. It is therefore responsible for the increased risk of coastal flooding and storm surges in the area. This situation attests to the impacts of climate change on flooding.

In Ghana, the spatial variation in response to climate change is affirmed by the works of Abbam, Johnson, Dash & Padmadas (2018) and Larbi, Nyamekye, Dotse, Danso & Annor, (2022). The former found out that the climate of Ghana has become prone to droughts due to increasingly drier climate over the last century. The most affected areas are in the Northern, Upper East and Upper West Regions. On the other hand, the latter investigated temperature and rainfall projections and their impacts on stream flow under different climate change scenarios in the Tano River Basin in Ghana. They found a general no significant increase in rainfall but significant increase in temperature. These changes had a corresponding decrease in mean annual streamflow for Tano River, suggesting more chances of drought than flooding.

In the Volta Lake, Amisigo, Logah & Obuobie (2018) (2018) projected an increase in rainfall under A1B and A2 IPCC special report emission scenarios (SRES) with a corresponding increase in average annual inflow to the Volta Lake by about 17% and 16% respectively, suggesting a potential for flooding. These findings therefore imply mixed impacts of climate change on water resource systems in Ghana, with the potential for both droughts and floods. They thus suggest that for a disaster risk management purposes studies must be localised at basin levels.

According to Reisinger et al. (2020), flood disaster risk is defined with regards to impacts of the flood and responses of a particular system to the impacts. It is, therefore, dependent on the factors that influence the flood as a hazard and its characteristics on one hand, and vulnerability on the other hand (Bagewadi, 2017; Kang et al., 2018). Flood hazard is influenced by climatic and anthropogenic activities, which define its generation, magnitude, frequency and severity. Vulnerability, on the other hand, is dependent on the characteristics of a system that make particular elements susceptible to the effects of flooding (Dolan & Walker 2006; Phongsapan et a., 2019). For a social system like coastal communities, vulnerability is determined by physical, social, economic, political and other environmental factors (Aman et al., 2019; Hadipour et al., 2020; Maanan et al., 2018 and Rocha et al., 2020).

2.8 Vulnerability Assessment

Different sectors and research communities (e.g. disaster risk management, food security, livelihoods security, health, climate change, and environmental change) have used the term ‘vulnerability’ differently to suit their objectives (Füssel, 2007). However, the UNISDR (2009) defines

vulnerability as the 'characteristics and circumstances of a community, system or asset that make it susceptible to the damaging effects of a hazard'. The Coastal Zone Management Subgroup (CZMS) of the IPCC defines vulnerability in relation to hazards that are relevant to coastal areas, namely climate change and SLR. It however, still refers to the characteristics of the coastal area that determine its degree of being affected by the impacts of climate change and SLR and be unable to cope with the impacts (Godschalk & Burns, 2019).

The review of available literature reveals two distinct concepts; natural science and social science concepts that describe vulnerability (Hadipour et al., 2020). The former concept defines vulnerability as the predisposition of exposed systems or elements, for example people, farmlands, houses to flood hazards (Field et al., 2012). Based on this focus, vulnerability is frequently described only in terms of the physical susceptibility of the items at risk, for example, flood depth. In this regard, the extent of damage is measured quantitatively, through the use of a vulnerability curve, which is constructed based on depth-damage relationship (Merz et al., 2010). The natural science-based concept, however, limits the actual scope of vulnerability because it fails to take into account the ability of the elements that are at risk to resist damage or reduce impacts. For example, a house built of cement blocks with a raised building foundation will be less sensitive to the impacts of flood inundation than a house built of clay with unraised foundation, given the same depth of flood event.

The social science concept, on the other hand, describes vulnerability as an integration of characteristics that are inherent to the element at risk, such as

a community or household, prior to a hazard event (Hadipour et al., 2020). Unlike the physical science concept, social science concept considers the prevailing conditions of the element in relation to the characteristics of the hazard to determine the possible impact, thus, measuring the degree to which the element can be affected.

Despite the existing diversity based on the sector, and concepts governing the concept of vulnerability, Tompkins & Mileti (2005) distinguish three models for describing vulnerability that cut across sectors and conceptual point of view. The first model is the risk – hazard model, which conceptualizes vulnerability as the dose – response relationship between an exogenous hazard to a system and its adverse effects. The second is the social constructivist model. This model views vulnerability as condition of a household or a community that is determined by socio-economic and political factors that determine its sensitivity and adaptive capacity to a hazard.

The third concept, which is also a working concept for the Intergovernmental Panel on Climate Change (Kontogianni, Damigos, Kyrtzoglou, Tourkolias & Skourtos, 2019) defines vulnerability in relation to the impacts of climate change. In this regard, vulnerability is an integrated measure of the expected magnitude of adverse effects to a system caused by a given level of external stressors. This model considers vulnerability as being dependent on sensitivity and adaptive capacity of a system, which are intrinsic to the system.

Many studies have directly or indirectly been conceptually based on the interaction of sensitivity and adaptive capacity of a system to the impacts a hazard in defining vulnerability. For example, in assessing the levels of

vulnerability and flood risk in the Ankobra estuary in Ghana, Osmanet al. (2016) based their study on the interaction of hazard, exposure and vulnerability and adaptive capacity. In the conceptualisation, vulnerability was to a larger extent considered separate from the adaptive capacity and did not explicitly consider sensitivity, perhaps because both capacity and sensitivity are more intrinsic than exogenous to the element being considered, unlike hazard and exposure. However, factors such as household savings and community participation were considered as the determinants of coping capacity, while income, age, gender and education were considered as factors contributing to social vulnerability. Also, physical parameters, such as materials and condition of one's house, and the elevation of a particular area, which by their nature define the exposure of the community, were considered. The parameters, however, implicitly covered both sensitivity and the adaptive capacity, which are the integral elements of vulnerability. According to Marzi et al. (2019), age and gender contribute to individuals' sensitivity to the damaging impacts of a hazard, while income, savings and community participation contribute to their capacity to cope with the impacts of a hazard.

Different methods have been used for identification and isolation of sensitivity and adaptive capacity variables, which have been instrumental in understanding vulnerabilities of different systems to impacts of various hazards in most disaster risk studies. These include Analytical Hierarchy Process (AHP) and Principal Component Analysis (PCA) that are used to construct vulnerability indices that enable the quantification and visualisation of vulnerability.

2.8.1 Principal Component Analysis

Principal component analysis (PCA) is a multivariate technique for analysing data in which observations are characterized by numerous quantitative dependent variables that are correlated with one another (Abdi & Williams, 2010). According to Kim et al. (2021) PCA is one of the reliable modern data analysis techniques used for the construction of indices, which can be applied to determine the weights of specific variables and components. By combining different indicators, it efficiently recognises data patterns and minimises loss of information (Kim et al., 2021). This makes it possible to effectively identify the most important variables that determine a particular outcome. The relative significance of a component is obtained by calculating a ratio of the squared factor score of a particular observation by the eigenvalue associated with that component (Abdi & Williams, 2010). Since the goal of PCA is to extract the most important variable (factor) it focuses on calculating weights of the identified component. Kim et al. (2021) summarises the steps as involving creating correlation matrices for the variables, determining the major component (PC) loading from the matrices, and calculating eigenvalues and eigenvectors that help explain the variances measured. Equation 1 is then used to calculate scores to represent the weights of each variable (Kim et al., 2021)

Equation 1: $$W_{ij} = \frac{c_i v_j}{\sum_{i=1}^{n} \sum_{j=1}^{m} c_i v_j}$$

Where *n* represents the number of variables selected from principal components, and *m* is the number of selected principal components. In addition, c_i is the principal component loadings of the *i*th variable, and v_j is the variance explaining the *j*th principal component. The technique has been used

in similar studies, studies such as drought vulnerability assessment (Kim, 2019), to identify the principal variable that measures the level of vulnerability of a phenomena.

2.8.2 Analytical Hierarchical Process

Analytical Hierarchical Process (AHP), developed by Saaty (1977), is a multiple-criteria method that is based on the requirement for making a decision among a list of competing variables over a particular goal. It seeks to measure how significantly the predetermined set of variables influences an outcome. With an emphasis on the logical consistency and correlation of the factors that are compared throughout the entire hierarchical process, the choice is typically based on the perception of the key informant individuals (Kumar et al., 2021). Comparisons are made between pairs of structure elements at each level of the hierarchy, where the choices of the decision maker are presented using Saaty scale of relative importance (Hadipour et al., 2020). The scale uses numeric values ranging from 1 to 9, where 1 means that the variables being compared are equally important, 3 means that there is moderate advantage of one variable relative to the other, 5 means one variable is strongly favoured relative to the other, 7 means that one variable is strongly favored and has domination in practice, relative to the other variable, and 9 means that there is overwhelming evidence and facts about variable making it extremely favored in comparison with the other. The even values, 2, 4, 6 and 8 denote intermediate advantages between the odd values.

The application of the method enables comparison of qualitative variables and produce quantitative outputs regarding the importance of competing variable in influencing a particular dependent outcome (Kumar et

al., 2021). Owing to its flexibility and abilities, AHP has been extensively used in environmental, social and sustainability studies, for example, Hadipour et al. (2020).

According to Pachemska et al. (2014), the allocation of values to the variables in the AHP follows four principles. These are principle of reciprocity, which states that if variable *X* is *n* times more important than variable *Y*, variable *Y* is the *1/n* times more important element of *X*; principle of homogeneity, which states that comparisons are sensical only if the variables are of the same nature and are comparable; principle of dependence which ensures contrasting variables from the lower level with those from the upper level. Lastly, the principle of expectation, which ensures that once there has been a change made to the hierarchy's structure, a fresh estimate of the priorities must be made.

Central to AHP is the use of pairwise comparison matrix (PCM) to compare the weight of each of the variables. The quality of outputs is measured by a consistency ratio (CR) which measures the consistency of PCM, calculated by Equation 2 by Wu et al. (2016). According to Wu et al. (2016) for an accurate and consistent weighting of processes, CR should not exceed 10%.

Equation 2: $$CR = \frac{CI}{RI}$$

Where CR is the consistency ration. Table 1 is used to determine RI, which is a random index dependent on the number of criteria (N) that are being compared (Pachemska et al., 2014).

Table 1: Values for the random index (RI) for particular number of criteria (N)

N	1	2	3	4	5	6	7	8	9	10	11
RI	0	0	0.58	0.9	1.12	1.24	1.32	1.41	1.45	1.49	1.51

Source: Pachemska et al. (2014)CI is the consistency index which is calculated using Equation 3.

Equation 3: $$CI = \frac{\lambda_{max} - n}{n-1}$$

Where λ_{max} and n are the maximum eigenvalue and order of matrix, respectively.

2.9 Physical and socio-economic determinants of coastal vulnerability

Prior to running an AHP, variables that affect an output need to be identified. The review of available literature identified various physical and socio-economic variables that determine coastal vulnerability. Table 2 is a presentation of the common variables that determine coastal vulnerability. The variables have either increasing effect (+) or reducing effect (-) on coastal vulnerability. For example, an increase in flood inundation, wave height and tide range increase the vulnerability of coastal communities to flooding, while an increase in elevation and distance to coast lines decrease the level of expected vulnerability. Regarding social variables, ages below 18 years and above 65 and female sex increase vulnerability, while high level of employment, education and cohesion reduce vulnerability.

Table 2: Common variables that determine coastal vulnerability

Risk component	Sub-component	Variables	Proxy measure	Impacts	Reference
Hazard		Flood inundation		+	Hadipour et al. (2020)
Physical vulnerability/ Exposure		Wave height Tide range		+	Boateng et al. (2016), Hadipour et al. (2020), Evadzi et al. (2017), , Gornitz et al. (1994)
		Elevation Distance to coastline		–	Boateng et al. (2016), Hadipour et al., (2020)
Social vulnerability	Sensitivity	Population	Population density (%)		Hadipour et al. (2020)
		Age	Less than 16 years		Hadipour et al. (2020)
			More than 65 years	+	Hadipour et al. (2020) Marzi et al. (2019), Osman et al. (2016)
			Less than 16 years	+	
		Sex	% of female	+	Hadipour et al. (2020) Marzi et al. (2019), Osman et al. (2016)
	Adaptive capacity	Employment	Employment %	-	Dolan & Walker (2006), Hadipour et al. (2020) Marzi et al. (2019)
		Education	% of people with higher education	-	Hadipour et al. (2020) Marzi et al. (2019), Osman et al. (2016)
		Cohesion	High level of cohesion	-	Hadipour et al. (2020), Marzi et al. (2019), Osman et al., 2016)
		Access to resources	High access to resources	-	Hadipour et al. (2020), Marzi et al. (2019), Osman et al. (2016), Ribot, (1995)

Source: Compiled by the researcher based on literature review

CHAPTER THREE

MATERIALS AND METHODS

3.1 Research design

The study was driven by a positivist worldview. According to Creswell and Creswell (2018), the positivist worldview holds a deterministic philosophy in which causes determine the outcomes. Regarding coastal flood risk, the study assumed that there are factors that determine the flood risk, and understanding their dynamics can help understand the level of risk involved. By implication, changes in the factors will determine change in risk levels. According to Hadipour et al. (2020) and Rocha et al. (2020), flood risk is a function of flood hazard interacting with exposure and vulnerability of elements at risk. In addition, exposure and coastal vulnerability of coastal elements to flooding are influenced by both geophysical and socio-economic parameters (Ahsan & Warner, 2014; Aman et al., 2019; Boateng et al., 2016; Cutter et al., 2003; Fekete, 2009, Ge et al., 2017 and Maanan et al., 2018).

The mixed methods design was adopted in which both quantitative and qualitative data were collected and analysed to assess climate and LULC change impacts on coastal flood risk in the ACA. Different methods of data collection and analyses were employed based on data requirement of the specific objectives.

3.2 Study Area

The selected study area is located in the Western Region of Ghana (Figure 2). The area comprises the Ankobra River Basin (ARB) and the Ankobra River Basin Coastal Area (ACA) (shown in Figure 2). ARB shares boarders with Pra River Basin, Tano River Basin and the Gulf of Guinea to the

east, west and south respectively. It is located within latitudes 4°52´N and 6°27´N and longitudes 1°42´W and 2°33´W. It has an estimated total area of about 8,403 km^2 (Owusu et al., 2016). Climatically, the basin is situated in the south-western equatorial and the wet semi-equatorial climatic regions. The former is the wettest climatic region in Ghana with an annual mean rainfall above 1,900 mm. The basin experiences a bimodal rainy season , with a major season observed from March to July, and a minor season from September to October (Osei et al., 2021). The basin is covered with rainforest and semi-deciduous forest. The average annual temperature varies from 25° C cover highlands and forest regions to 27° C cover other areas of the basin.

The ACA is the area that is below a 30-meter contour line encompassing a 10 km^2 section of the Ankobra estuary. The estuary is largely located in Ellembelle district within latitudes 4°54´N and 4°53´N, and longitudes 2°15´W and 2°17´W, flowing into the Gulf of Guinea on the south (Osman et al., 2016). The main economic activities along the drainage system include both legal and illegal gold mining, cash crop farming and fishing.

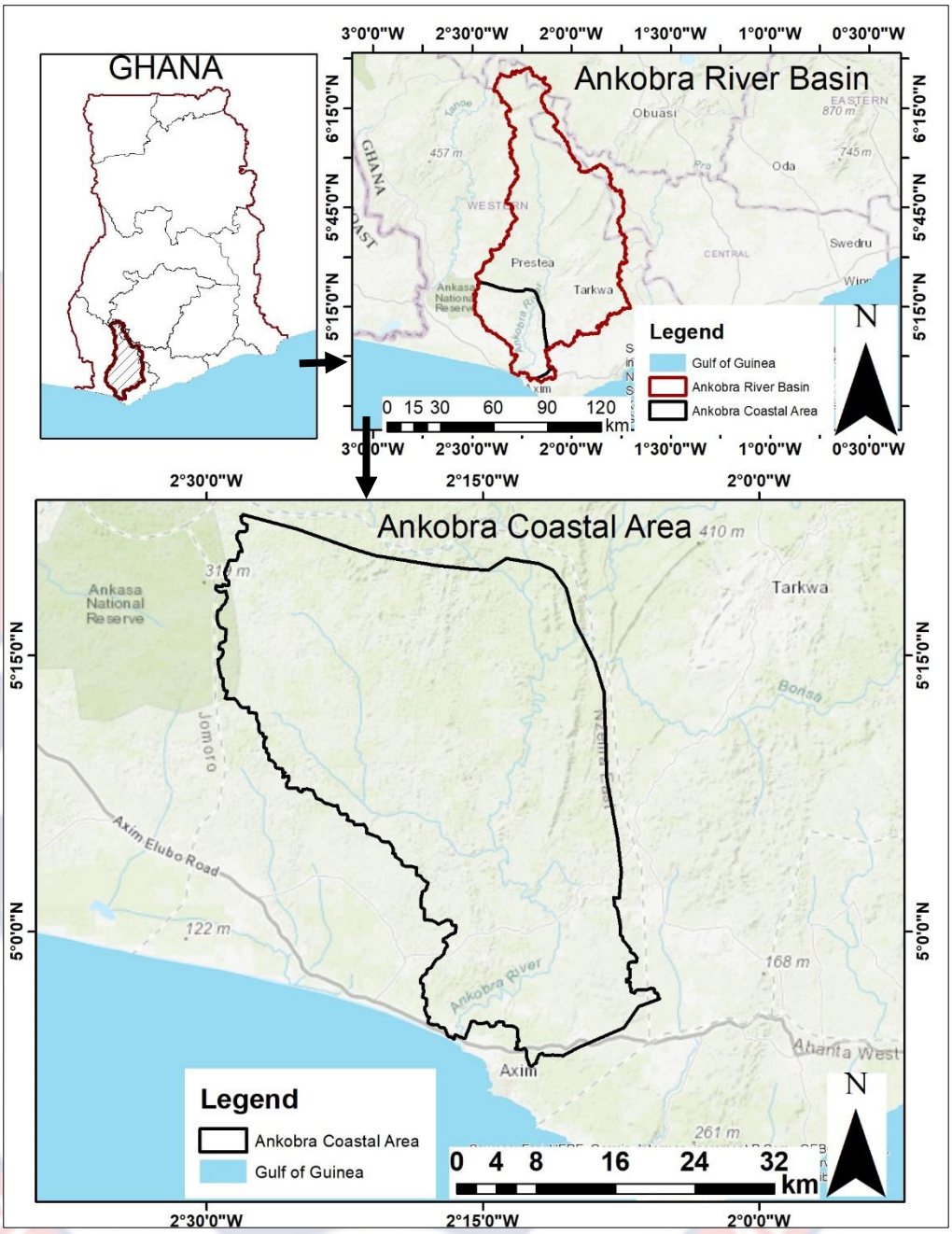

Figure 2: Map of study area showing the Ankobra Rier Basin (Above) and the Ankobra Coastal Area (Below)

Sources: Compiled by the researcher.

3.3 Data Acquisition

Data acquisition involved collection of satellite data, climatic data, socio-economic data and hydrological data. Different procedures and data

collection tools were therefore used. The following sections outline data acquisition procedures based on the type of data an analyses required.

3.1.1 Satellite data

The assessment of land use and land cover change is essential to assessing changes in water yield from a particular basin, owing to the critical role land use and land cover play in the hydrological process at basin level (Berihun et al., 2019; Gashaw et al., 2018; Kenea et al., 2021). To do this, the study used Landsat satellite images that depict past status of the basin, spanning from 1991 to 2022. The period was divided into four segments, 1991, 2008, 2016 and 2022.

For this objective, the study used satellite images from Landsat 4-5 for 1991 and Landsat 7 ETM for 2008, 2016 and 2022. The images with spatial resolution of 30 m were downloaded from Earth Explorer, an online portal of the United States Geological Survey (USGS) accessed through https://earthexplorer.usgs.gov/. The resolution and the atmospheric noise effects, such as cloud cover are known to affect the quality of the images. In this study, images with cloud cover of not more than 20% were selected. These factors, and image availability for some particular dates, influenced the choice of the assessment years. This approach was also used by Rwanga & Ndambuki (2017). Table 3 summarises the characteristics of the satellite images used in the study.

Table 3: Characteristics of satellite images used in the study

Path/Row	Landsat	Sensor	Spatial Resolution	Number of bands	Year and Date of acquisition
194/056	L 4-5	TM	30m	6	22 January 1991
194/057	L 4-5	TM	30m	6	22 January 1991
194/056	L 7	TM and TM+	30m	8	23 January 2008
194/057	L 7	TM and TM+	30m	8	23 January 2008
194/056	L 7	TM and TM+	30m	8	6 January 2016
194/057	L 7	TM and TM+	30m	8	6 January 2016
194/056	L 7	TM and TM+	30m	8	6 January 2022
194/057	L 7	TM and TM+	30m	8	29 January 2022
194/057	L 7	TM and TM+	30m	8	29 January 2022

Source: Compiled by the researcher from https://earthexplorer.usgs.gov/

3.1.2 Temperature and Rainfall Data

Temperature and rainfall data were assessed to determine changes or variations in them. This was important for the estimation of the impact of temperature and rainfall on flood risk in the Ankobra River Basin Coastal Area (ACA).

Secondary data, in terms of historical time series data for temperature and rainfall from 1986 to 2020 were used. Data for 3 stations located in the basin (as indicated in Table 4) were acquired from the Ghana Meteorological Agency (GMET).

Table 4: Particulars of climate data for the basin

Basin Station	Latitude	Longitude	Elevation (m)	Period of focus	
				Rainfall	Temperature
Benso	05°09´0N	01°54´0W	170.8	1986-2019	2000-2013
Bogoso	05°24´0N	02°02´0W	82.3	1986-2014	
Sefwi Bekwai	06°12´0N	01°54´0W	60.1	1986-2020	1986-2020

Sources: Compiled by the researcher based on data acquired from GMET

3.1.3 Socio-economic Data

Vulnerability assessment focused on households located in the ACA, covering parts of Ellembelle and Nzema East Districts in Ghana. The ACA was defined according to the criteria of Patel, Jain, Patel & Kalubarme, (2021). Since the study aimed at understanding the socio-economic characteristics of the households, it involved household heads as the primary participants.

Vulnerability assessment in the ACA aimed at mapping out areas of low, medium and high vulnerability to floods based on socio-economic and physical variables. For socio-economic variables, sex, age, education, access to productive resources, affiliation to groups and physical condition of houses were considered, on which data was collected. Similar studies in a similar set up as Ankobra River Basin also used these variables as key determinants of household vulnerabilities to floods including Hadipour et al. (2020), Marzi et al. (2019) and Osman et al. (2016). Physical variables considered include coastal elevation, distance to coastline, rate of SLR, mean wave height (MWH) and mean tide range (MTR), as used by Boateng et al. (2016), Hadipour et al. (2020) and Evadzi et al. (2017).

3.1.3.1 Sampling procedures

Sample size was calculated using Cochran's equation (Equation 4) at 95% confidence level and 30% degree of variability. The equation is appropriate for use where population size are either large or not known (Halim & Hasnita ., 2017; and Naing, 2003), which was the case with the Ankobra River Basin, where there was no population framework, and population size was therefore not known. Degree of variability of 30% was used because the population in the coastal zone in Ankobra River Basin is regarded homogenous (Naing, 2003 & Osman et al., 2016). Finally, systematic random sampling as used by Espina (2018), was employed in selecting individual households, from whom data was collected through interviews

Equation 4: $$n_o = \frac{Z^2 pq}{\varepsilon^2}$$

Where n_o is the minimum returned sample size, Z is from tables and equal to 1.96 at 95% confidence level, p is the degree of variability, which was economically set at 0.3, q = 1-p, while Ɛ , is the margin of error = 5%. Based on this, the minimum number of households selected to be interviewed were 323 ($n_o = 323$).

3.1.3.2 Data collection instruments

Data collection involved stratification of the area to ensure spread and representativeness across the basin, which was key for vulnerability mapping and classification of flood risk areas across the basin. In this regard, three strata, lower, middle and upper were delineated. Stratification was mostly informed by distance to the coastline because it is one of the factors that determine coastal vulnerability (Boateng et al. 2016). Further to this, the major economic activities differ across the span of the coastal area, with those close

to the ocean being more reliant on fishing than the those away from the ocean (Osman et al., 2016). The lower strata comprised households located 0 to 15 km from the coastline on-land, while the middle and the upper strata comprised communities from 15 km to 30 km and 30 to 44 km from the coast line respectively. Thirty percent of the communities, chosen at random, within each stratum were selected to participate in the study. Based on this, 3 communities, 2 communities and 1 community were selected to participate in the lower, middle and upper strata respectively.

Sampling of households for interviews was done using systematic random sampling as used by Espina (2018) to identify actual households heads who were then subjected to interviews using an interview guide.

3.1.4 Soil and Water Assessment Tool (SWAT) Model Data

The SWAT model is used to estimate hydrological outputs from a basin in response to changes in parameters that affect water balance in a particular basin. It has been widely used in studying hydrological responses to changes in climate and land use land changes (Gashaw et al. 2018; Kenea et al., 2021). The SWAT model requires historical weather data, digital elevation models (DEM) and soil data for the study area as input parameters to generate stream flow and water yield, among many other parameters as outputs. In addition to these data sets, SWAT requires stream flow data for calibration and validation of the model.

Weather data, which includes daily rainfall, temperature, evapotranspiration, solar radiation, wind and relative humidity were sourced from the Ghana Meteorological Agency (GMET) for the weather stations at Benso and Sefwi-Bekwai in the Ankobra River Basin for the period between

1986 and 2021. To ensure a satisfactory network of weather stations, four more stations were introduced in the Basin. One at Bogoso, where GMET has a station but whose data were incomplete, characterised by too many gaps, and three other stations as presented in Table 5. Data for the introduced stations were sourced from an online portal of the National Aeronautics and Space Administration (NASA) POWER Project of the United States Federal Government, accessed on https://power.larc.nasa.gov/data-access-viewer/. Relatedly, climate data from the NASA POWER project were also used in similar studies by Larbi et al. (2022) in Tano River Basin in Ghana.

Table 5: Particulars of the Meteorological stations

Meteorological Station	Assigned Number	Latitude	Longitude	Elevation (m)	Period
Benso	WS01	5°9′0N	1°54′0W	48.97	1986-2021
Bogoso	WS02	5°24′0N	2°1′48W	100.69	1986-2021
Sefwi Bekwai	WS03	6°12′0N	1°45′0W	152.29	1986-2021
Prestea	WS04	5°27′0N	2°7′0W	100.69	1986-2021
Station 5	WS05	5°23′2N	2°20′2W	97.30	1986-2021
Station 6	WS06	5°9′0N	2°22′1W	39.91	1986-2021

Sources: Compiled by researcher based on data acquired from GMET and https://power.larc.nasa.gov/data-access-viewer/

Digital elevation model (DEM) data for the basin was accessed from Earth Explorer, an online United States Geological Survey (USGS) DEM data portal on https://earthexplorer.usgs.gov/, acquired by the Advanced Spaceborne Thermal Emission and Reflection Radiometer Version 3 (ASTER V3), in the form of a raster file. It has 1 arc-second latitude and longitude postings (~30 m) and employs cloud masking to avoid cloud-contaminated pixels. The data has a resolution of 30 m. DEM data sources from USGS has been widely used for similar studies, for example, Abrams et al. (2020).

Soil data was downloaded from FAO and UNESCO online portal on https://www.fao.org/soils-portal/data-hub/soil-maps-and-databases/ in the form of Digitalised Soil Map of the World (DSMW), a raster file. FAO soil data have been widely used in similar studies, for example kin studies by Larbi et al. (2022) and Kenea et al. (2021). Stream flow data were sourced from the Hydrological Services Department of the government of Ghana, measured at the Prestea gauge station which is located on 5°27′0N latitude and 2°7′0W longitude. It is about 62 km upstream of the discharge point of the Ankobra River Basin into the Atlantic Ocean. The station is therefore a discharge point of the upstream sub-basins covering a total area of 4358.6 km^2 of the total Ankobra River Basin area of 8457.4 km^2.

3.4 Data Preparation

3.4.1 Satellite Data

Satellite images were processed in ENVI 5.3. Practically, the processing of the images involved compositing, mosaicking, extraction, atmospheric correction and making subsets of areas of interests for land classification. Subsets were then exported to ArcMap 10.4.1. Supervised land classification was done using Maximum Likelihood Classification (MLC) algorithms in ArcMap. According to Gevana et al. (2015), supervised LMC is regarded a more robust approach for land use classification using remotely sensed images. This approach has been in a study by Kenea et al. (2021).

3.4.2 Temperature and Rainfall data

Data processing was performed in Microsoft Excel 2016. It involved arranging the data in a format for use in R, and calculating monthly averages. The data was further analysed with the R Studio. Prior to trend test, the data

was checked using autocorrelation coefficient function (ACF), in R. This was necessary to inform appropriate trend test package to use for analysis in R, that is, either, *pcbw* or *mkttest* packages. *Pcbw* package is used when there is no autocorrelation in the data, while *mkttest* is applicable where autocorrelation exists.

3.4.3 Socio-economic data

Preparation of socio-economic data involved checking for consistency and completeness, coding and data entry into SPSS software (Version 25). It also involved ranking of the physical and socio-economic factors based on similar studies, for example Aman et al. (2019), Boateng et al. (2016), Ge et al. (2017), Hadipour et al. (2020), Maanan et al. (2018) and Rocha et al. (2020). They were ranked on a scale of 1 to 5, where 1 represents very low contribution to coastal vulnerability, and 5 represents extremely high contribution to coastal vulnerabilities. This was essential for use in the analytical hierarchy process (AHP). Table 6 and Table 7 show the rankings for socio-economic and physical variables respectively.

Table 6: Ranking of socio-economic variables for determining vulnerability

	Very Low (1)	Low (2)	Moderate (3)	High (4)	Very High (5)
Sex		Male		Female	
Age (years)	<16	18-35	35-50	50-65	>65
Education	Tertiary	Upper secondary	Lower secondary	Primary	No formal education
Income (US$)	>4.9	3.91-4.9	2.91-3.9	1.91-2.9	0-1.9
Access to productive assets	Access with ownership rights		No ownership but access rights		No access and no ownership rights
Affiliation to social groupings		Yes		No	
Height of house foundation (m)	> 1.0 m above the ground	0.5 m to 1.0 m above the ground	0.3 m to 0.5 m above the ground	>0 to 0.3m above the ground	Ground level

Source: Compiled by researcher from *Aman et al. (2019)*, Boateng et al. (2016), Ge et al. (2017), Hadipour et al. (2020), Maanan et al. (2018) and Rocha et al. (2020).

Table 7: Ranking of physical variables for determining vulnerability

	1: Very Low	2: Low	3: Moderate	4: High	5: Very High
Coastal elevation (m)	>10	10 to 6	6 to 4	4 to 2	<2
Distance to coastline	≥1000	200 to 1000	50 to 2000	20 to 50	≤20
SLR rate (mm/year)	<0.5	0.5 to 1.5	1.5 to 2.5	2.5 to 3.5	>3.5
MWH (m)	<0.3	0.3 to 0.6	0.6 to 0.9	0.9 to 1.2	>1.2
MTR (m)	>5	3.5 to 5	2 to 3.5	1 to 2	<1

Source: Compiled by researcher from Aman et al. (2019), Boateng et al. (2016), Ge et al. (2017), Maanan et al. (2018) and Rocha et al. (2020).

3.4.4 SWAT Model data

3.4.4.1 Preparation of Digital Elevation Model (DEM) data

Digital Elevation Model (DEM) raster image was uploaded into ArcMap 10.4.1. The image was filled using the spatial analyses tools to enhance the quality by removing any imperfections in the image, and clipped using data management tools to extract area of focus covering the Ankobra River Basin. Figure 3 shows a filled DEM clipped to the extent of the Ankobra River Basin

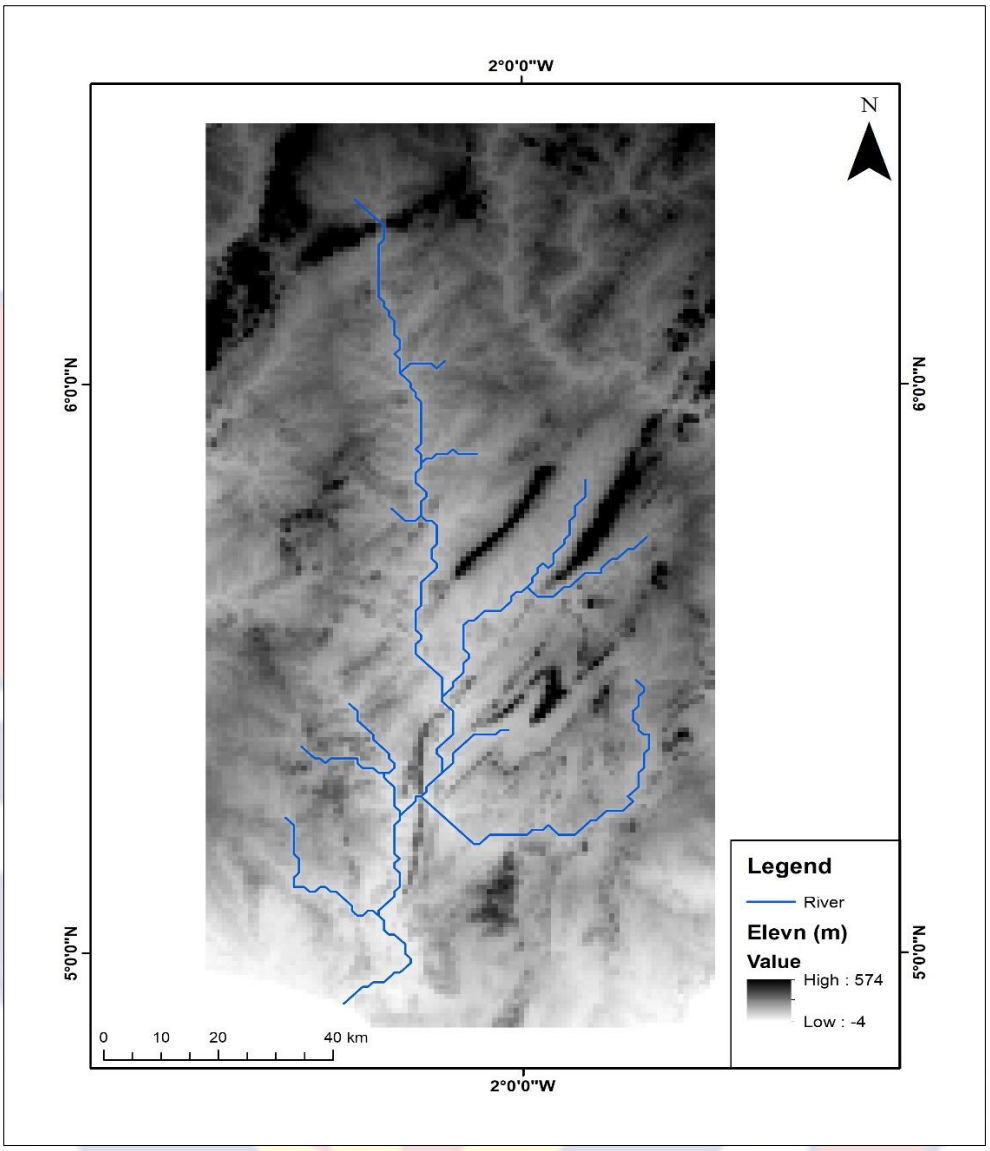

Figure 3: Digital Elevation Model (DEM) data extracted for SWAT input
Source: Compiled by researcher SWAT Model outputs based on DEM acquired from https://earthexplorer.usgs.gov/

3.4.4.2 Preparation of land use data

Preparation of the land use data involved development of a LULC map and lookup table for input in SWAT model. Land use land cover map for 2016 (Figure 4) was used as land use data input. The year 2016 was chosen because it falls within the period, which experienced the highest rate of LULC changes in the Ankobra River Basin, as observed in objective 1.

From the map, a text look-up table was developed based on the land classes and their respective area. The look-up table, with four land use types was created (Table 8) and linked to SWAT by recoding the land classes with nomenclature compatible to SWAT2012 database.

Table 8: Land use look-up table for SWAT input

Value	Land use name	Description
1	WATR	SWAT Code for water, and depicting land covered by water
2	URMD	SWAT Code for urban medium-density depicting land covered by buildings or made bare for other purposes, such as roads, markets, mining etc.
3	FRST	SWAT Code for dense vegetation and depicting land covered by thick woody vegetation.
4	FRSE	SWAT Code for sparse vegetation and depicting land covered by shrubs, annual agricultural crops and grass.

Source: Compiled by the researcher

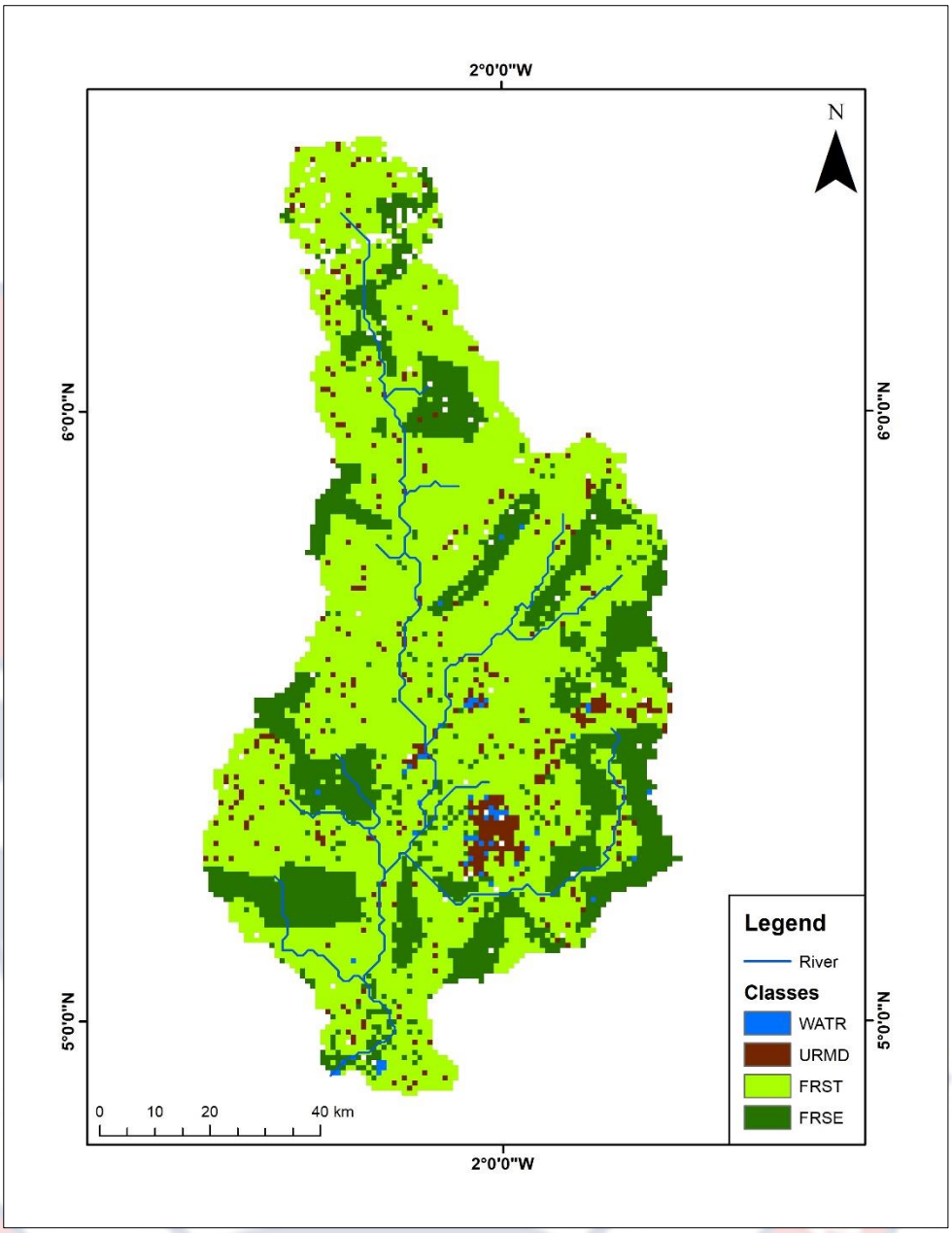

Figure 4: Land use map for the Ankobra River Basin prepared for SWAT input

Source: Produced by the researcher in ArcMap 10.5

3.4.4.3 Preparation of soil data

Preparation of the soil data involved development of a soil map and lookup table for SWAT model input. To do this, FAO soil map was put into ArcMap 10.4.1 as a raster feature, and was projected accordingly. The map extent that covers the Ankobra basin was extracted by masking using spatial

analyst tools and using the Ankobra River Watershed polygon as the feature mask data. Details of the soil classes were defined from the attribute table of the clipped map and linked with SWAT database to enable SWAT read the soil look-up table. A text file of look up table (Table 9) was prepared from the data attribute table of the soil classes for the basin. This was then linked with SWAT by editing the SWAT2012 user soil database.

Table 9: Soil use look-up table for SWAT input

Value	Name	Description
1	Ao1-ab-1046	Sandy clay loam soil with low hydraulic conductivity
2	Ao29-b-1054	Loam soil with low hydraulic conductivity
3	Ao7-ab-1067	Sandy clay loam soil with high hydraulic conductivity
4	Fx1-b-1184	Sandy loam soil with high hydraulic conductivity
5	Nd8-b-1573	Loam soil with high hydraulic conductivity

Source: Compiled by the researcher based on soil data acquired from based on soil data acquired from https://www.fao.org/soils-portal/data-hub/soil-maps-and-databases/

3.4.4.4 Preparation of weather data

Daily weather data was prepared in Microsoft Excel, which involved the arrangement of the records into a format compatible with SWAT database. The data was then entered into SWAT weather data generator (WGEN) from which a user database for aligning weather parameter inputs and SWAT database was generated. The outputs from the WGEN were then used to edit the weather database in SWAT12. This allows SWAT to read individual weather parameters from individual weather stations in the basin.

3.5 Data Analysis

3.5.1 Land use land cover change analysis

3.5.1.1 Land cover classification

Land cover classification was based on the Food and Agriculture Organisation (FAO) land cover classification scheme and adopted from Anderson et al. (1972). The basin was explored using google earth, with a background expert knowledge of the basin acquired through field visits. Four classes were defined for classification as shown in Table 10. At least 20 training samples for each land use class were taken, from which training signatures were created to inform the MLC algorithms. The choice of number of samples was based on the size and spread of a class in question. In practice, the more the samples, the better the system identifies pixels that belong to a particular class in the classification processes.

3.5.1.2 Accuracy assessment and change detection

The accuracy of land classification was assessed using the error matrix method, which displays overall performance accuracy, Kappa statistics and producer´s and user´s accuracy as described by Kindu et al. (2013) were generated. Classification accuracy explains the degree of difference between the real physical image and the classified image (Hussein et al., 2020). Accuracy values, measured by Kappa statistics, and producer´s and user´s accuracy of 100% depict perfect classification accuracy, and no accuracy when the value is 0% (Hadi et al., 2014; Hussein et al., 2020; Kindu et al., 2013). User´s and producer's accuracies are proportions of number of correctly classified pixels to the total number of classified pixels a particular class added in row and columns respectively in a matrix.

Table 10: Land Use Classification Scheme Adopted from FAO Land Classification System

Class	Land use	Description
Class type I	Water	All land extent covered by water
Class type II	Developed area and Bare land	All land extent that has been modified by human activities rendering them bare or built up
Class type III	Dense Vegetation	All land extent covered by thick woody vegetation
Class type IV	Cultivated and Sparse vegetation	All land extent covered by sparse vegetation, agricultural activities and shrubs, depicting transformation from dense vegetation

Source: Adapted from Anderson et al. (1972)

The overall accuracy, on the other hand, is the proportion of correctly classified pixels to the total number of reference pixels. Kappa coefficient was calculated from the user´s and producer´s accuracies. Change in a particular land cover was calculated using Equation 5, adopted from Kindu et al. (2013).

Equation 5: $$LULC\ Change\ (\%) = \left[\frac{Area_{Final\ year} - Area_{Initial\ year}}{Area_{Initial\ year}}\right] * 100$$

Where *Area* is extent of each LULC type. Positive and negative values of LULC respectively indicate an increase and decrease in the extents of each LULC type.

3.5.1.3 Temperature and rainfall change analysis

The temperature and rainfall data of the study were analysed to determine trends using Mann-Kendall trend statitistical test (Equation 6) a non-parametric method for detecting trends in hydro-meteorological time series data (Hirsch et al., 1984), and calculated as;

Equation 6: $$Z = \begin{cases} \frac{S-1}{\sqrt{VAR(S)}} & if\ S > 0 \\ \frac{S+1}{\sqrt{VAR(S)}} & if\ S < 0 \\ 0 & if\ S = 0 \end{cases}$$

Where S is the Mann-Kendal Statistic calculated as:

$$S = \sum_{k=1}^{n-1} \sum_{j=k-1}^{n} Sign(x_j - x_k)$$

VAR (S) is the variance of S, and is calculated as:

$$VAR\ (S) = \frac{1}{18}[n(n-1)(2n+5) - \sum_{p=1}^{g} t_p(t_p - 1)2t_p + 5)]$$

The Mann-Kendal Trend Test value (Z) indicates an increase in the variable if it is more than zero ($Z > 0$), and a decrease in the variable if it is less than zero ($Z < 0$). Given a confidence level α, the observation is statistically significant if $|Z|$ is more than $Z(1-\alpha/2)$, where $Z(1-\alpha/2)$ is the corresponding value of $P=\alpha/2$ following the standard normal distribution. In this research, a confidence level, α, of 0.05 was used and $|Z|$ was considered significant if it is more than $|1.96|$ as described and used by Arrieta-Castro et al. (2020).

3.5.1.4 Vulnerability analysis

Frequencies for the variables sex, age, education, access to productive resources, affiliation to groups and condition of houses for each of the sampled communities were calculated using Statistical Package for Social Sciences (SPSS v.25). The variables were then weighted using AHP. AHP uses pairwise comparison matrix (PCM) to compare the weight of each of the parameters in achieving an objective. The quality of outputs from the process was measured based on the consistency ratio (CR). A CR of less than 0.1 implied that the comparison of the variables was consistent and acceptable (Hadipour et al., 2020 & Wu et al., 2016). The weighted variables were then used to calculate social and physical vulnerability indices using the Square Root of Product Mean as used by Tano et al. (2018), and presented in Equation 7. All calculations were performed in Microsoft Excel version 2016.

Equation 7: $$VI = \sqrt{\left[\frac{1}{N}\sum_{i=1}^{N} x_i\right]}$$

Where *VI* is physical or social vulnerability index; *N* is the number of variables; *x* is the weighted physical or social variable. Lastly, the calculated vulnerability indices were used to produce vulnerability maps using krigging analyst tool in in ArcMap 10.4.1.

3.5.2 Hydrological modelling and flood mapping

3.5.2.1 Watershed delineation

Watershed delineation is a process of setting boundaries within which hydrological processes take place and where modeling in SWAT will focus. This involved setting a SWAT project in ArcMap, after which digital elevation model (DEM) was set up by uploading the DEM raster file and projecting it accordingly. A DEM-based stream definition was then performed to create streams and outlets. A watershed outlet was selected at the discharge point of the Ankobra River into the Atlantic Ocean. Finally, sub-basin parameters were calculated.

3.5.2.2 Hydrological Research Unit (HRU) analysis

The Hydrological research unit (HRU) analysis involved defining land use, soil and slope parameters, as well as HRU definition in the model. This was done by putting land use and soil map along with their look-up tables that were prepared prior to HRU analysis based on the SWAT2012 database that was used in the SWAT Model. Two classes of slope were set, with one ranging from 0 % to 1 % and the other at more than 1 %. Regarding HRU definition, a multiple HRU criteria was set with thresholds of land use percentage over sub-basin area, soil class percentage over land use area and slope class percentage over soil class area set at 20%, 10% and 20%,

respectively as recommended by the SWAT user's manual for most common applications in modelling social and water attributes of a basin (Kenea et al., 2021). These were, therefore, adopted since there has been no localised studies done to determine the best thresholds for the Ankobra River Basin.

3.5.2.3 Weather data input

This involved inputting weather parameters to complement soil and land cover data in the analysis process. It involved inputting details for the weather stations, followed by uploading data for rainfall, temperature and relative humidity. Solar radiation and wind speed meters were set at simulation, which enables SWAT to simulate the parameters based on weather and weather station parameters.

3.5.2.4 Calibration, validation and model performance evaluation

Model calibration was done in SWAT-CUP 5.1.6.2 using SUFI1 calibration method. Basin management, basin processes, reach and soil parameters that relate to stream flow were set. The period for simulation was set to begin from 2003 to 2008, using data observed at the Prestea gauge station. Five hundred (500) simulations were run. There was a reiterative process of changing the parameters that affect stream flow until a satisfactory model was calibrated. The performance of the model was manually evaluated using the Nash-Sutchiffe coefficient (NSE) and performance bias (PBIAS) in Microsoft Excel. NSE was used to determine the appropriateness of the model, while PBIAS was used to determine whether the model overestimates or underestimates the observations as used by Kenea et al. (2021).

NSE and PBIAS were calculated as:

Equation 8: $$NSE = 1 - \frac{\sum_{t=1}^{T}(Q_m^t - Q_o^t)^2}{\sum_{t=1}^{T}(Q_o^t - \bar{Q}_o)^2}$$

Equation 9: $$PBIAS = \frac{\sum_{t=1}^{T} 100(Q_m^t - Q_o^t)}{\sum_{t=1}^{T}(Q_o^t)}$$

Where Q_o^t is the observed flow at a given time, Q_m^t is the modelled flow at a given time and $\bar{Q}_o$ is the mean observed flow. A value of NSE of above 0.5 indicates a satisfactory model performance while a good model has an NSE value of above 0.75 (Kenea et al., 2021). A positive value of PBIAS indicates an underestimation of observations while a negative value indicates overestimation of the observations by the model. Validation was performed using data from 2013 to 2019. The choice of the calibration and validation periods was based on the completeness of observed data. The period that had no missing data was chosen.

3.5.2.5 Mapping of flood risk in the Ankobra Coastal Area

This involved extraction of peak water yields for 1991, 2008 and 2021 from SWAT outputs. These were used to delineate all areas equal to or less than the yield using raster calculator in the map algebra expression function of the raster calculator spatial analyst tool in ArcMap 10.4.1. A 30-meter resolution DEM was used, and was filled before use. Filling is a process of removing elevation gaps and was performed using fill function in the hydrology spatial analyst tool. All areas with elevation equal to or less than the peak water yield were regarded prone to inundation from the hydrological processes in the ARB. From these, flood inundation maps for 1991, 2008 and 2021 were developed. The flood inundation maps were then superimposed on the vulnerability maps to generate a flood risk map.

CHAPTER FOUR

RESULTS

4.1 LULC Changes in the ARB between 1991 and 2022.

4.1.1 Land use land cover change

The study found that four major land use land cover classes; water, developed/ bare land, cultivated/sparse vegetation, and dense vegetation dominate in the basin. Figure 5 shows the dominating land use land cover classes in the ARB between 1991 and 2022. The area covered by the observed land use land cover classes varied between 1991 and 2021 with recorded changes taking place in all the land use land cover classes over the period (for additional information see Table 11).

Specifically, dense vegetation cover decreased from 3844.5 km^2 in 1991 to 2075.97 km^2 in 2022 representing a 46 % loss. Also, there was variation in observed changes across the period. The area covered by dense vegetation decreased from 3844.5 km^2 in 1991 to 2267 km^2 in 2008 representing a loss of 41 %. It however, increased to 2530.3 km^2 in 2016, representing 12 % gain between 2008 and 2016 followed by a decrease to 2075.97 km^2 in 2022 representing 18 % loss. The rates of change in dense vegetation cover in the basin were -92.76 km^2/year, 32.84 km^2/year and -75.71 km^2/year between 1991 and 2008, 2008 and 2016, and 2016 and 2022 respectively. Therefore, the highest loss (-41 %) and gain (12 %) in dense vegetation cover occurred between 1991 and 2008, and 2008 and 2016 respectively.

Also, cultivated and sparse vegetation cover was 4365 km^2 in 1991 and increased to 5599.17 km^2 in 2022 representing a net gain of 28 % over the

period. There were variations in the state of land use and rate of change across the period. The total area covered by cultivated/sparse vegetation increased from 4365 km^2 in 1991 to 5831 km^2 in 2008 representing a gain of 34 % over the period. It however decreased to 5221.6 km^2, representing a loss of 10 % between 2008 and 2016, and then increased to 5599.17 km^2 in 2022, representing a gain of 7 % between 2016 and 2022 (Table 11). The rate of change in sparse vegetation varied across the segments. It increased at a rate of 86.24 km^2 per year between 1991 and 2008 and assumed a negative trend at a rate of -76.18 km^2 per year between 2008 and 2016. It then increased at a rate of 62.9 km^2 per year between 2016 and 2022.

Additionally, built-up/bare land increased by 959 % between 1991 and 2022, with variations in the extent of cover and rate of change across the period. The area covered by either buildings or road infrastructure was 45.31 km^2 in 1991 and increased by 112 % in 2008, 289 % between 2008 and 2016, and by 23 % between 2016 and 2022. The rates of land transformation to built-up/bare land were 3.25 km^2/year, 36.3 km^2/year and 14.83 km^2/year between 1991 and 2008, 2008 and 2016, and 2016 and 2022 respectively. Thus, the highest modification (289 %) with buildings or clearing rendering the land bare for different uses took place between 2008 and 2016.

Further, Table 11 indicates that land covered by water increased by 98.69 km^2 representing 845 % between 1991 and 2022 in the ARB with variations. In 1991, land covered by water was 11.68 km^2, and increased to 67.54 km^2, 122.73 km^2 and 110.37 km^2 in 2008, 2016 and 2022 respectively. These represented a change of 478 %, 83 %, and -11 % between 1991 and 2008, 2008 and 2016, and 2016 and 2022 respectively. (Table 11).

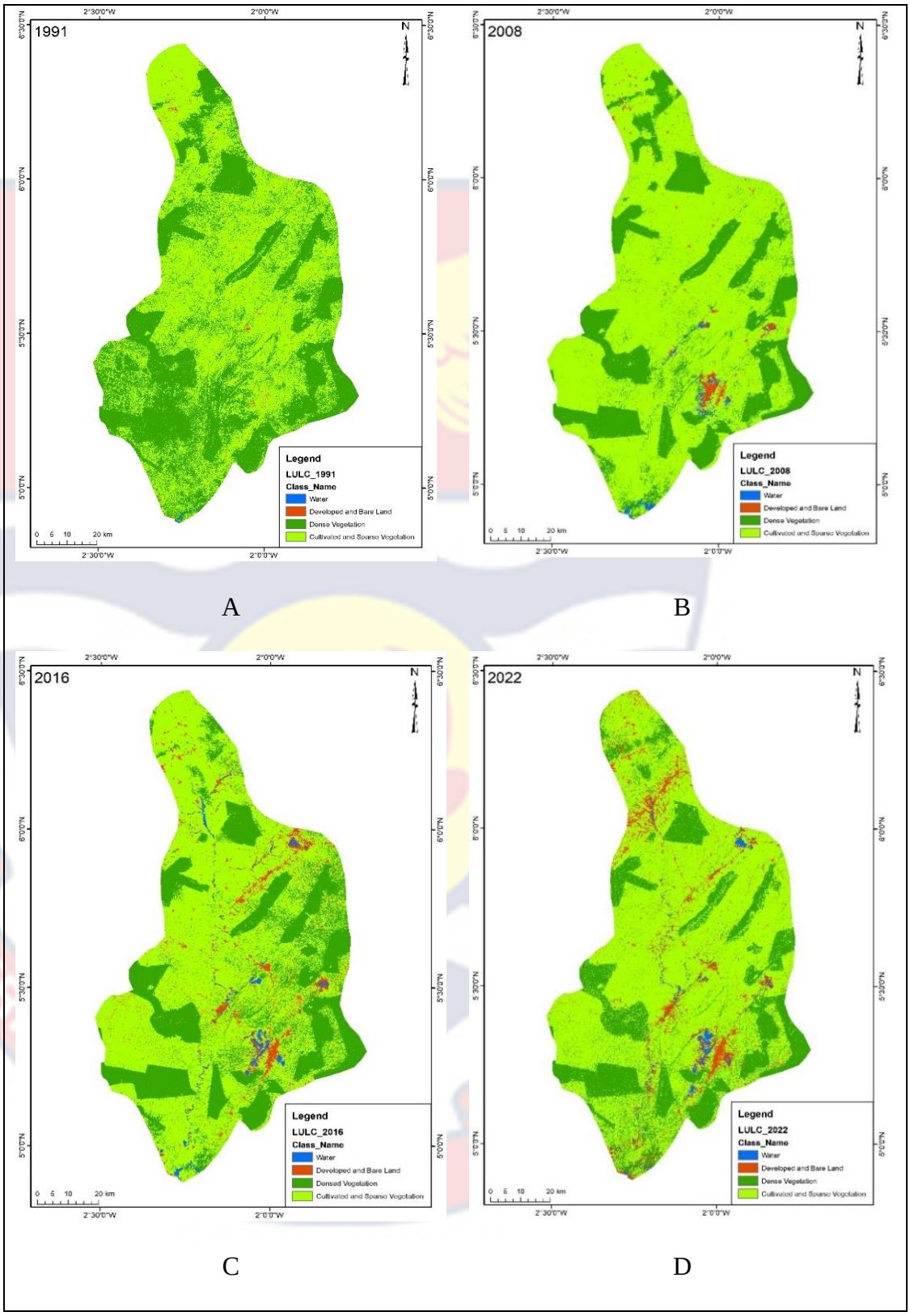

Figure 5: LULC maps for Ankobra Basin in 1991 (A), 2008 (B), 2016 (C) and 2022 (D)

Source: Produced by the researcher in ArcMap 10.5

Table 11: Land Use change in Ankobra Basin between 1991 and 2022

Class	Area (km^2)				Changes							
					2008-1991		2016-2008		2022-2016		2022-1991	
	1991	2008	2016	2022	Area (km^2)	%	Area (km^2)	%	Area (km^2)	%	Area (km^2)	%
Water	11.68	67.54	123.73	110.37	55.86	478	56.19	83	-13.36	-11	98.69	845
Developed area and Bare land	45.31	100.56	391.22	480.05	55.25	122	290.66	289	88.83	23	434.74	959
Dense Vegetation	3844.50	2267.5	2530.3	2075.97	-1576.9	-41	262.72	12	-454.28	-18	-1768.50	-46
Cultivated and Sparse vegetation	4365.00	5831.00	5221.6	5599.17	1466	34	-609.40	-10	377.57	7	1234.13	28

A negative sign (-) denotes a decrease in area of land use cover in a succeeding year of analysis. A positive value denotes an increase in area of land use cover in a succeeding year of analysis
Source: Compiled by the researcher based results of land use change analysis

4.1.2 Land use land cover transition

Figure 6 shows the transition and variations of land use between 1991 and 2022. Generally, the study shows a loss in dense vegetation and a gain in sparse vegetation, bare and developed land as well as areas covered by water over the study period. The highest loss in dense vegetation cover took place between 1991 and 2008, which is also the period that registered the highest gain in sparse vegetation cover. This implies a transformation of dense vegetation to predominantly cultivated and sparse vegetation. Between 2008 and 2016, there was some gain in dense vegetation cover and highest gain in developed/bare land at the expense of cultivated/sparse vegetation, implying that a portion of cultivated/sparse vegetation was transformed back to dense vegetation, while part of it was transformed to developed/bare land and water.

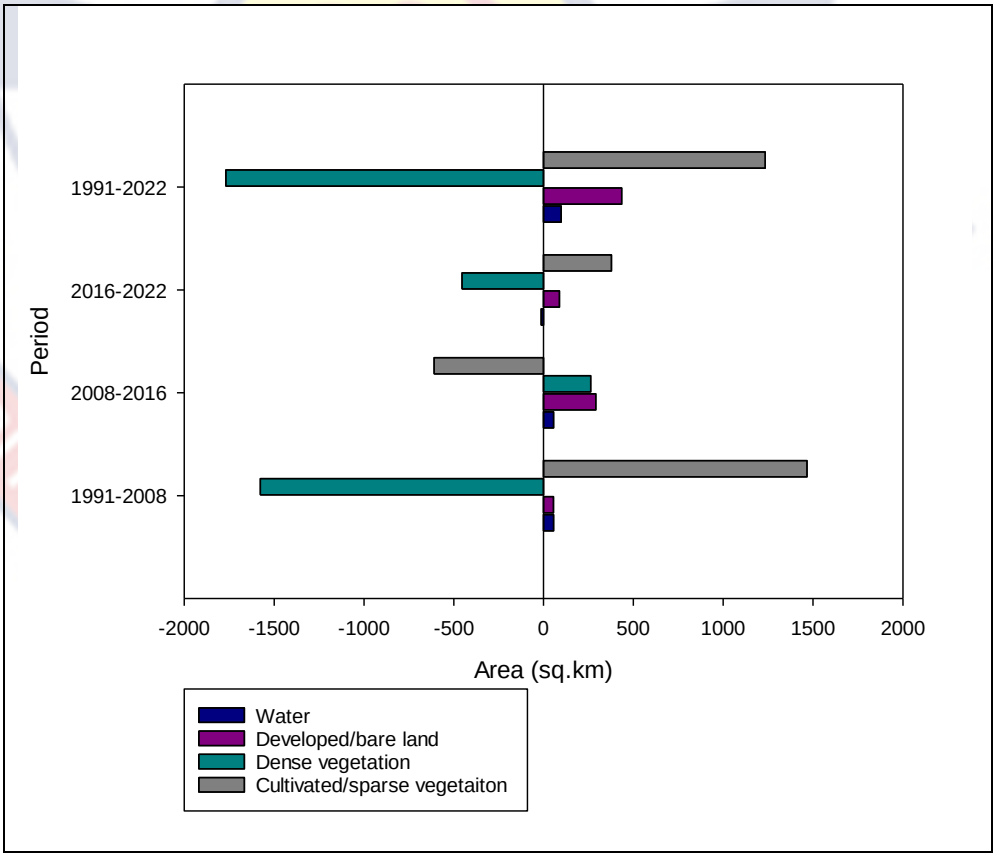

Figure 6: Land use transition for ARB between 1991 and 2022

Source: Produced by the researcher based on land use change analysis

4.2 Climate variability in the ARB between 1991 and 2021

Figures 7 and 8 show the long-term trends in temperature at Benso and Sefwi-Bekwai weather stations respectively, and show an increase in temperature observed at both stations. The observed increments in temperature are significant at 95% confidence interval, with Mann-Kendal trend test values (Z) of 2.34 and 3.39, respectively. Table 12 shows the actual changes observed at the two stations. Temperature increased by 0.9 °C between 2000 to 2013 at Benso station and by 1.1 °C between 1986 and 2020 at Sefwi-Bekwai station, representing 3.5 % and 4 % increase in temperature respectively. There are variations in monthly trends as shown in Figure 9. On the average, the highest significant increases in temperature were observed in July, October, November and December, while no significant increases were observed in February, April, May and June between 1991 to 2021.

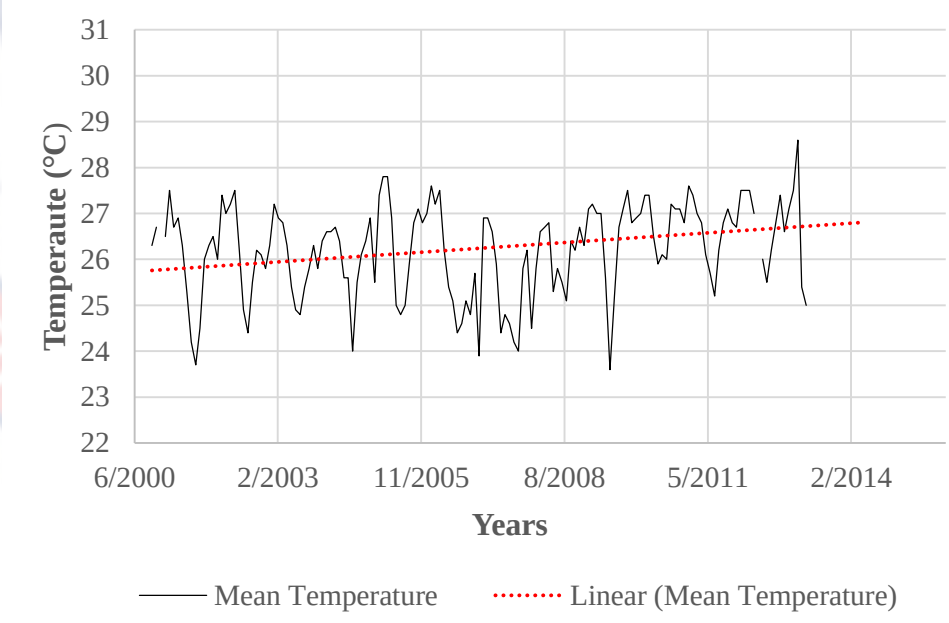

Figure 7: Temperature trend at Benso Meteorological station

Source: Produced by the researcher in R-studio based on data from GMET

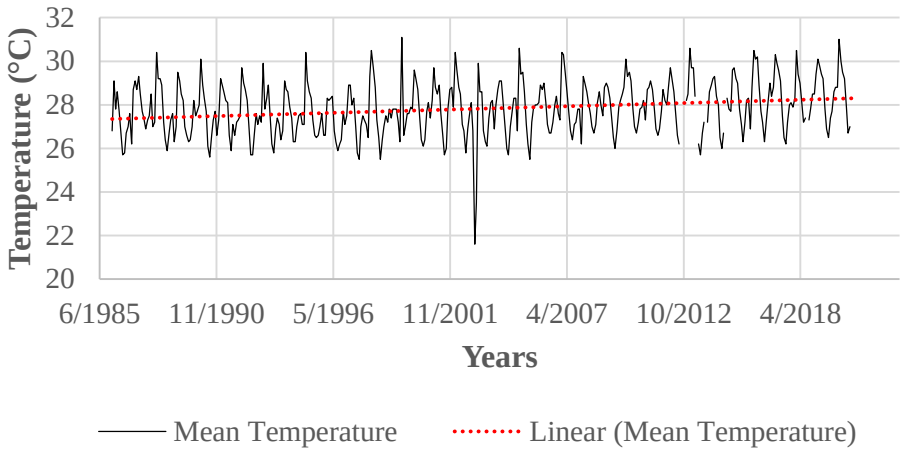

Figure 8: Temperature trend at Sefwi-Bekwai Meteorological station

Source: Produced by the researcher in R-studio based on data from GMET

Table 12: Temperature Change in the Ankobra Basin between 2000 and 2013 for Benso Station and 1986 to 2020 for Sefwi-Bekwai Station

Meteorological Station	Period (Years)	Change in temperature	% Change
Benso	2000-2013	0.9°C	3.47%
Sefwi Bekwai	1986-2020	1.1°C	4.01%

Source: Compiled by the researcher based on data from GMET

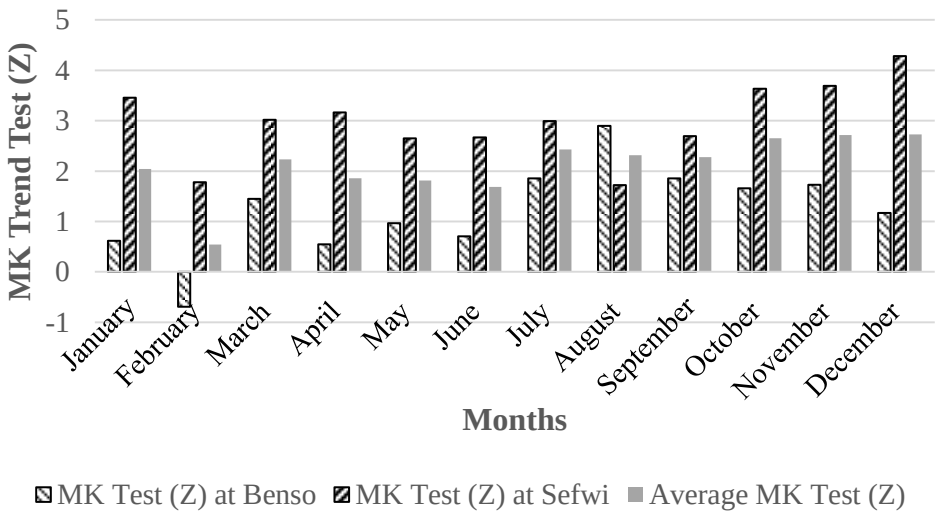

Figure 9: Monthly Mann-Kendall trend test for temperature at Benso and Sefwi-Bekwai Stations

Source: Produced by the researcher in Microsoft Excel 2016 based on data from GMET

Figures 10 and 11 show long term trends in rainfall at the Benso and Sefwi-Bekwai weather stations respectively. Both trends show increasing amount of rainfall over the period at the two stations. The recorded variation is significant at the Benso station whilst no significant increase in rainfall was measured at the Sefwi-Bekwai station at the 95 % confidence interval, with Mann-Kendal trend test values (Z_{MK}) of 2.67 and 0.77 respectively. Table 13 shows the actual change in rainfall registered at the Benso and Sefwi-Bekwai weather stations. The amount of rainfall increased by 35 % between 1986 and 2019 at the Benso weather station, and by 13 % between 1986 and 2020 at the Sefwi Bekwai station. There are observed variations in monthly amount of rainfall and between the 2 stations as shown in Figure 12. Significant increases in rainfall were observed in February and May between 1986 to 2020 at the Benso station. At Sefwi-Bekwai, significant decrease and increase in rainfall were observed in August and November respectively over the same period. On average, only May recorded a significant increase in rainfall in the ARB.

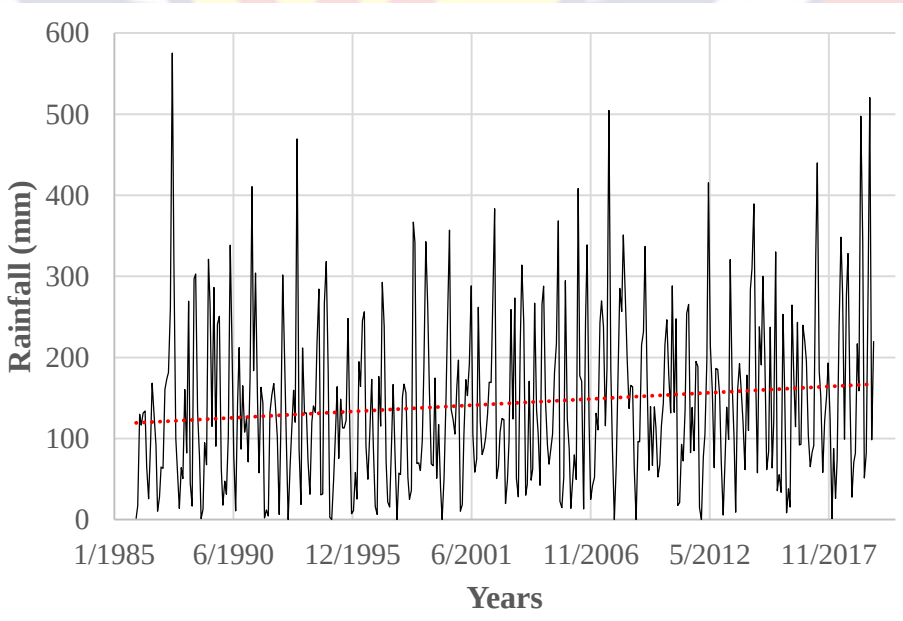

Figure 10: Rainfall trend at Benso weather station

Source: Produced by the researcher in R-studio based on data from GMET

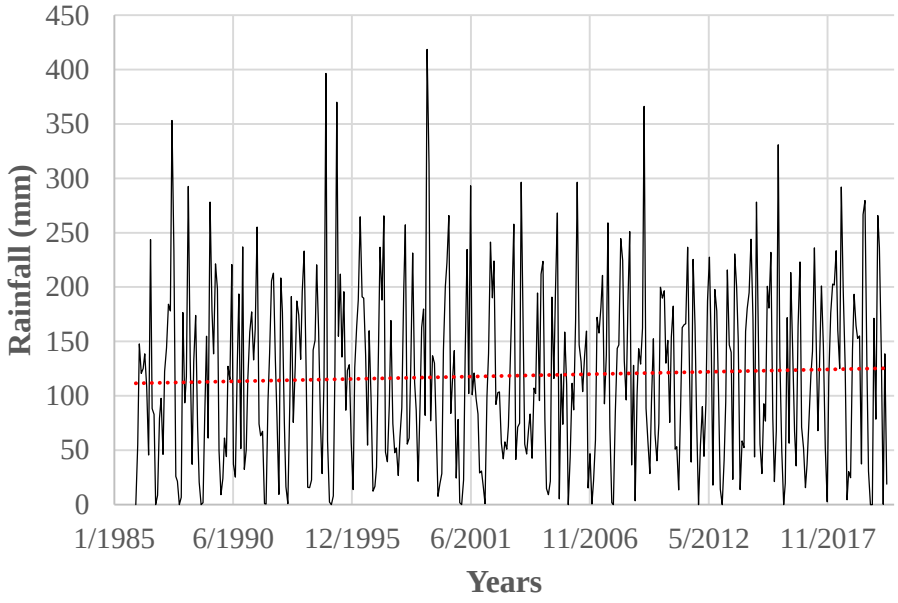

Figure 11: Rainfall trend at Sefwi Bekwai Meteorological Station

Source: Produced by the researcher in R-studio based on data from GMET

Table 13: Rainfall Change in Ankobra Basin, calculated based on linear trend line

Meteorological Station	Period	Change in Rainfall	% Change
Benso	1986-2019	42 mm	35 %
Sefwi Bekwai	1986-2020	13 mm	13 %

Source: Produced by the researcher in R-studio based on data from GMET

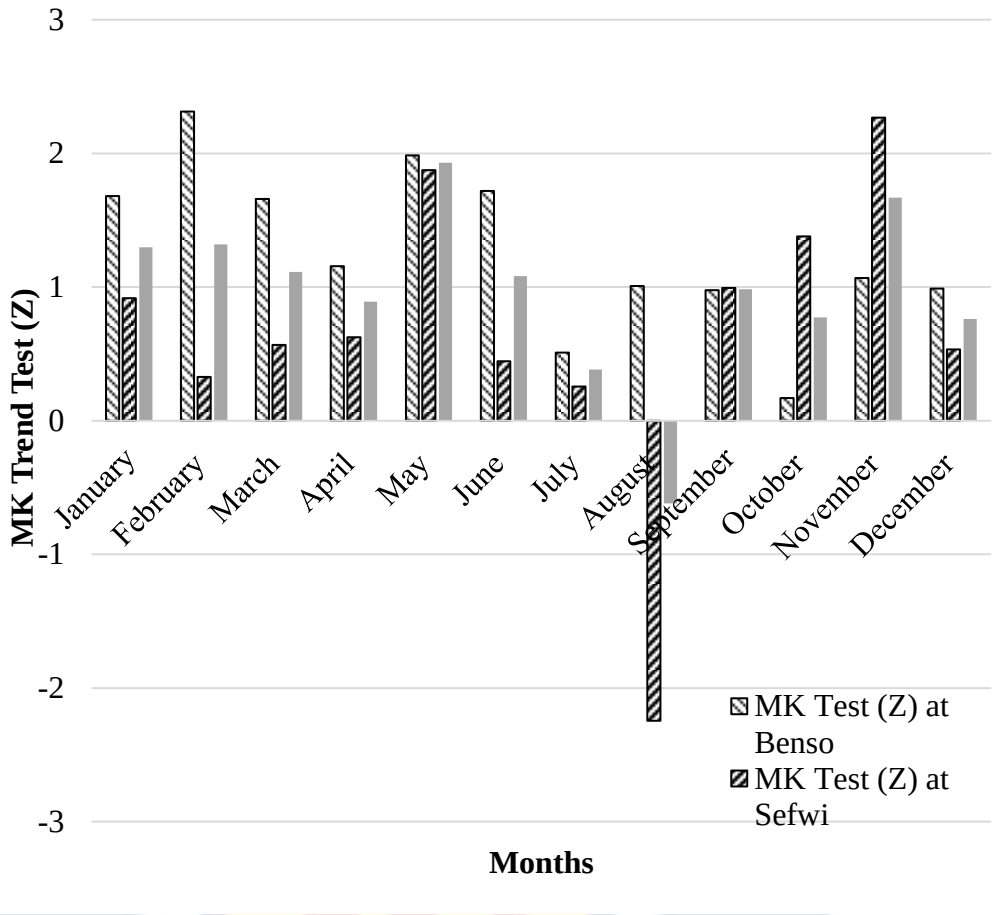

Figure 12: Monthly Mann-Kendall Trend test for Rainfall at Benso and Sefwi-Bekwai Stations

Source: Produced by the researcher in Microsoft Excel 2016 based on data from GMET

4.3 Vulnerability of the Coastal Area in the ARB to Flooding

4.3.1 Socioeconomic and physical characteristics of ACA

Table 14 shows the dominant socio-economic variables that characterise households in the ACA in the ARB, with focus on sex, age, education, income, access to productive natural resources, affiliation to social groups, and height of house foundations. It shows that the ACA is dominated by male headed households with a mean frequency of 61.1 ± 18.5 %. Minor variations exist across the south, central and northern sections of the area. The

southern section has male dominance of 53.4 %, while the central and northern sections have male dominance of 66.9 % and 59.1 % respectively.

In terms of age of the household heads, 75.6 % are aged between 30 to 65 years with standard deviation of 4.6. There are variations across the area, such that the southern part of ACA has 74.5 %, while the central and northern sections have 76.5 % and 75.0 % dominance of households' heads aged 30 to 65 years (Table 14).

Regarding education, the ACA is dominated by the household heads that attained up to lower secondary level of education. They account for 50.1 ± 11.1 % of the sampled respondents. There are also variations among communities situated in the southern, central and northern parts of the ACA with 50.3 %, 50.0 % and 50.0 % dominance of household heads with education level of up to lower secondary respectively. (Table 14).

Also, 97.0 (3.3 %) of the households in the ACA live below the absolute poverty line (APL). Disaggregating by sections, the study shows that there are more households leaving below APL in the northern section (100 %), followed by the central (98%) and least in the southern section (94%).

In terms of access to natural resources for production and livelihood support, the area is dominated by households that have unrestricted access to the resources with a mean frequency of 97.8 ± 2.1 %. The southern section has the highest access (99 %) and decreases northwards, central and northern sections having 97.9 % and 95 % dominance of households with unrestricted access to natural productive resource respectively.

Non-affiliation to social groups dominates the ACA. Over 69 % of the households do not have formal affiliation to social groups. Non-affiliation is

highest in the northern section, with 84.1 % of households having no formal affiliation to groups. The dominance decreases southwards, with 68.1 % in the central section and 63.8 % in the southern section.

Lastly, the table shows the structural condition status of houses with focus on height of foundations. The area is dominated with houses that have foundation with height of between 0.3 m and 0.5 m representing 57 ± 9.7 %. Variations however exist among the southern, central and northern sections of the area with dominance level of 60.3 %, 54 % and 70 % respectively.

Table 14: Frequency (in %) of socio-economic variables in ACA, and their ranking

Social economic variables	Sex	Age	Education level	Poverty level	Access to productive resources	Affiliation to social groupings	Height of house foundation
Dominating variable in the coastal area of the ARB	Male	30 -65 years	Lower secondary	Below absolute poverty line	Unrestricted access	Non-affiliation	0.3-0.5 m
Average for the ACA	61.1 ± 18.5	75.6 ±4.61	50.1 ± 11.1	97.4 ±3.3	97.8 ± 2.1	69.3 ±12.8	57.0 ±9.4
Northern section	53.4	75.0	50.0	100.0	95.0	84.1	70.0
Central section	66.9	76.5	50.0	98.9	97.9	68.1	54.0
Southern section	59.1	74.5	50.3	94.0	99.0	63.8	60.3
Vulnerability Ranking	2	3	3	5	3	4	3

Source: Produced by the Researcher based on descriptive analysis of primary socio-economic data collected from Ankobra Coastal Area

Table 15 shows the status of physical factors characterising the ACA according to past geophysical studies of the area, and *in situ* assessment using GIS applications. The elevation of the area ranges from -4m to 574 m relative to sea level. Longest distance from the coast line to the coastal zone line (outer boundary of the coastal area) is 42,000 m. Mean Wave Height (MWH) and Mean Tide Range (MTR) are 1.2 m and 1.0 m respectively.

Table 15: Magnitude of physical variables in ACA and their ranking

Physical variable	**Magnitude**	**Reference**	**Ranking**
Elevation (m)	-4 to 574		Varying
Distance to coastline (m)	0 to 42, 000		Varying
Mean Wave Height (m)	1.2	Boateng et al. (2016),.Evadzi et al. (2017), Rocha et al. (2020), Tano et al. (2018)	4
Mean Tide Range (m) State in full	1.0	Boateng et al. (2016),.Evadzi et al. (2017), Rocha et al. (2020), Tano et al. (2018)	4

Source: Deduced by the Researcher using GIS in ArcMap 10.5 and compiled from Boateng et al. (2016),.Evadzi et al. (2017) and Rocha et al. (2020), Tano et al. (2018)

4.3.2 Weighting of vulnerability variables

Table 16 shows the weighted criteria of each of the socio-economic and physical variables in influencing coastal vulnerability in ACA. The weights were calculated using AHP. Regarding socio-economic factors of coastal vulnerability to impacts of floods, the study shows that the house

condition and income level of a household have the highest and second highest criterial weights of 0.25 and 0.23 respectively. Affiliation to social groups was assigned the smallest weight in practices. Weighting of the physical variable using AHP Eigenvalue (λ_max) of 7.65 and consistency ratio of 0.08 are acceptable.

Regarding physical variables, elevation and MWH have the highest and second highest weighted criteria of 0.46 and 0.24 respectively. MTR and MWH have weight factors of 0.16 and 0.14 towards contributing to coastal vulnerability. Similarly, in practice, weighting of the physical variable using AHP had Eigenvalue (λ_max) of 4.12, and consistency ratio of 0.04 are acceptable.

Table 16: Weight of socio-economic and physical variables in influencing coastal vulnerability in ACA

Type of variables	Variable	Criteria weight
Socio-economic	Sex	0.08
	Age	0.14
	Education	0.13
	Income	0.23
	Access to Resources	0.12
	Affiliation to Social groups	0.06
	Height of House Foundation	0.25
Physical	Elevation (m)	0.24
	Distance to coastline (m)	0.46
	MWH (m)	0.14
	MTR (m)	0.16

Source: Calculated by the Researcher using AHP in Microsoft Excel 2016 based on physical and descriptive analysis of socio-economic vulnerability parameters

4.3.3 Vulnerability indices

Table 17 shows social and physical vulnerability indices calculated as square root of mean of product of magnitude of measure, ranking and criteria weight of each of the variables. They are disaggregated based on the location of the communities (i.e. the north, central and southern sections of the ACA). Social vulnerability indices range from 0.61 to 0.63, while physical vulnerability indices range from 0 to 0.94.

Table 17: Vulnerability Indices for the studied communities in the ACA

Section	Community	Social Vulnerability Index	Physical Vulnerability Index
North	Kotukromu	0.63	0.00
	Sika ne Asem	0.63	0.77
	Gyampre	0.63	0.00
Central	Sentum	0.62	0.69
	Ayawora	0.62	0.00
	Gwirabanso	0.62	0.77
	Akosuno	0.63	0.69
	Draw River	0.62	0.00
	Adibirim	0.62	0.00
	Anshiaem	0.62	0.69
	Asonti	0.61	0.69
	Akropong	0.61	0.00
South	Sanwohma	0.61	0.94
	Apataim	0.61	0.94
	Adelekezo	0.62	0.77
	Abu	0.61	0.00
	Bramianko	0.61	0.77
	Kokuaville	0.61	0.77
	Anyinasie	0.61	0.77

Source: Calculated by the researcher using Square Root of Product Mean in Microsoft Excel 2016 based on physical and descriptive analysis of socio-economic vulnerability parameters.

4.3.4 Vulnerability mapping

The social and physical vulnerability indices were used to produce vulnerability maps as shown in Figure 13. Social vulnerability indices (SVI) ranged from 0.61 to 0.63. In the study places with indices of less than 0.621 were classified as having low social vulnerability. Similarly, those areas with SVI between 0.621 and 0.630 were classified as of medium vulnerability while those areas with SVI more than 0.630 were classified as areas of high social vulnerability. Physical vulnerability indices (PVI) on the other hand, ranged from 0 to 0.94. In all, areas with PVI of less than 0.36, 0.63-0.76 and more than 0.76 were regarded to be of low, medium and high vulnerability to floods, respectively.

An overlay of SVI and PVI by fuzzing produced integrated vulnerability indices (IVI), such that all areas with IVI less than 0.28 were classified as low vulnerability, while those with IVI between 0.28 – 0.58 and more than 0.58 were classified as having medium and high vulnerability, respectively.

Figure 13 shows that social vulnerability is high in the northern section, medium in the central section, and low in the southern section of the ACA. Physical vulnerability, on the other hand, is highest in the southern section and decreases north-eastwards (Figure 13B). It is low in the north-western parts of the ACA. When overlaid, an integrated vulnerability map, which is shows that vulnerability is highest on southern section and decreases north-eastwards with the north-western parts of the ACA recording the lowest vulnerability index (Figure 13C). Table 18 shows the level of vulnerability of the coast communities based on social and physical factors.

Table 18: Level of Vulnerability for coastal communities based on social and physical factors

Level of vulnerability	Coastal Communities
High vulnerability	Kokuaville (Kokotre), Sanwohma Bokazo, Apa taim, Adelekezo, Bramiankor, Anyinase, Akesuno, Sentum, Gwira banso and Ashiaem
Medium vulnerability	Ankropong, Asonti, Gyampre and Sika ne Asem
Low vulnerability	Kotukromu , Ayawora, Adibrim, Abu

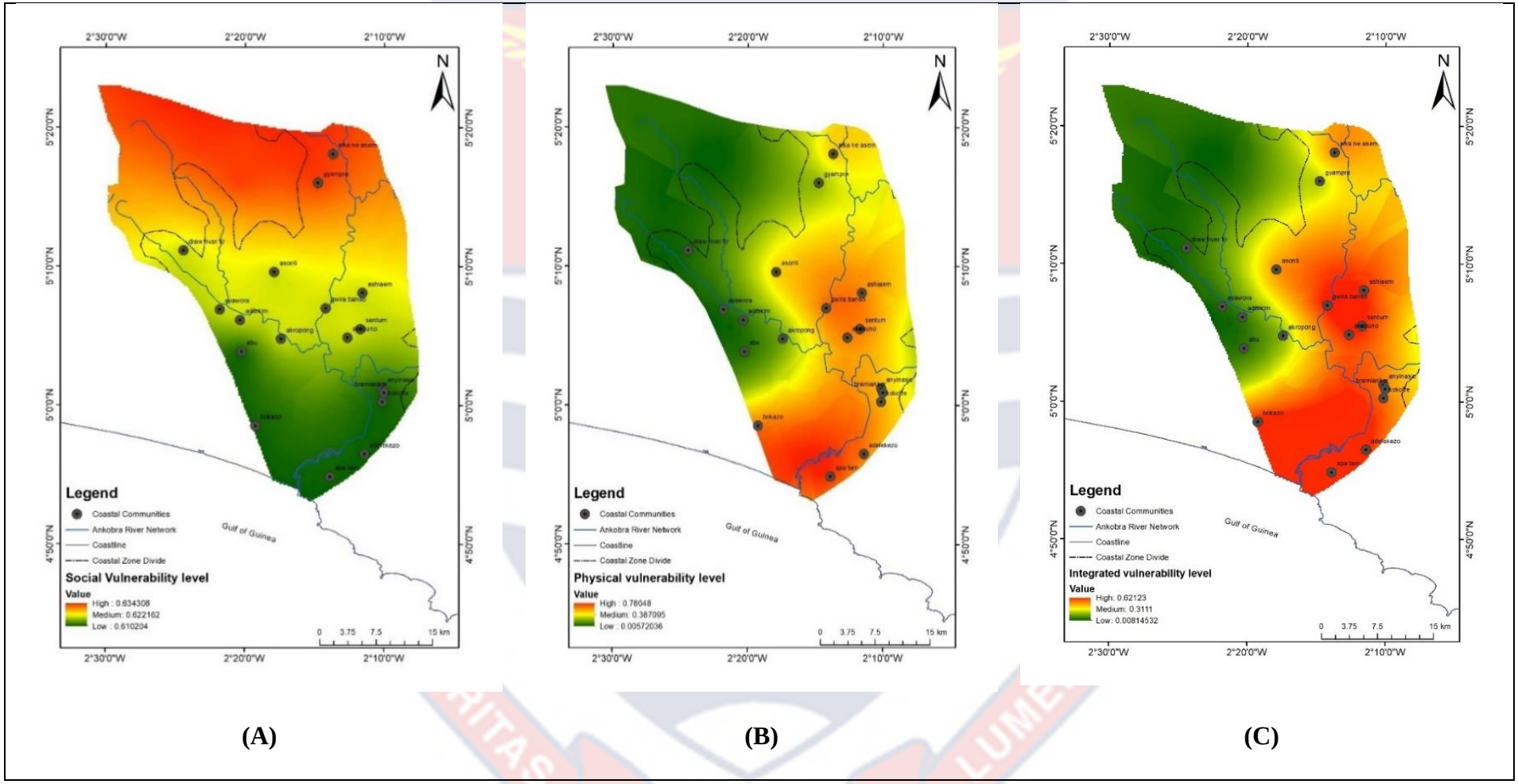

Figure 13: Index-based social (A), physical (B) and integrated (C) vulnerability maps of ACA

Source: Produced by the researcher in ArcMap 10.5 based on physical and social vulnerability indices in the ACA.

4.4 Extent of flooding due to climatic changes in the ACA

The purpose of this objective was to estimate the magnitude of inundation influenced by climatic and LULC changes in the basin. Hydrological modelling was used in SWAT and involved watershed delineation, HRU analysis, calibration, simulation and validation, model performance evaluation, and water yield prediction. The water yield prediction values were used to map the extent of inundation in the ACA

4.4.1 Watershed delineation and Hydrological Response Unit (HRU) analysis

Figure 14 shows the outputs from watershed delineation and hydrological response unit analysis performed in SWAT. Map A shows sub-basins of the ARB. The basin has a total of 23 sub-basins ranging from 28.67 km^2 to 1508.69 km^2, and a total area of 8457.38 km^2. Map B shows the soil composition of the basin. The basin is predominantly covered by sandy-loam soil (soil code number Fx1-b-1184) and sandy-clay soil (soil code number Ao7-1b-1067), covering 48.8 % and 34 % of total areas on the basin respectively. Over 87 % of the basin has a slope ranging from 0-1 %, while the rest has a slope of more than 1 % (Table 18).

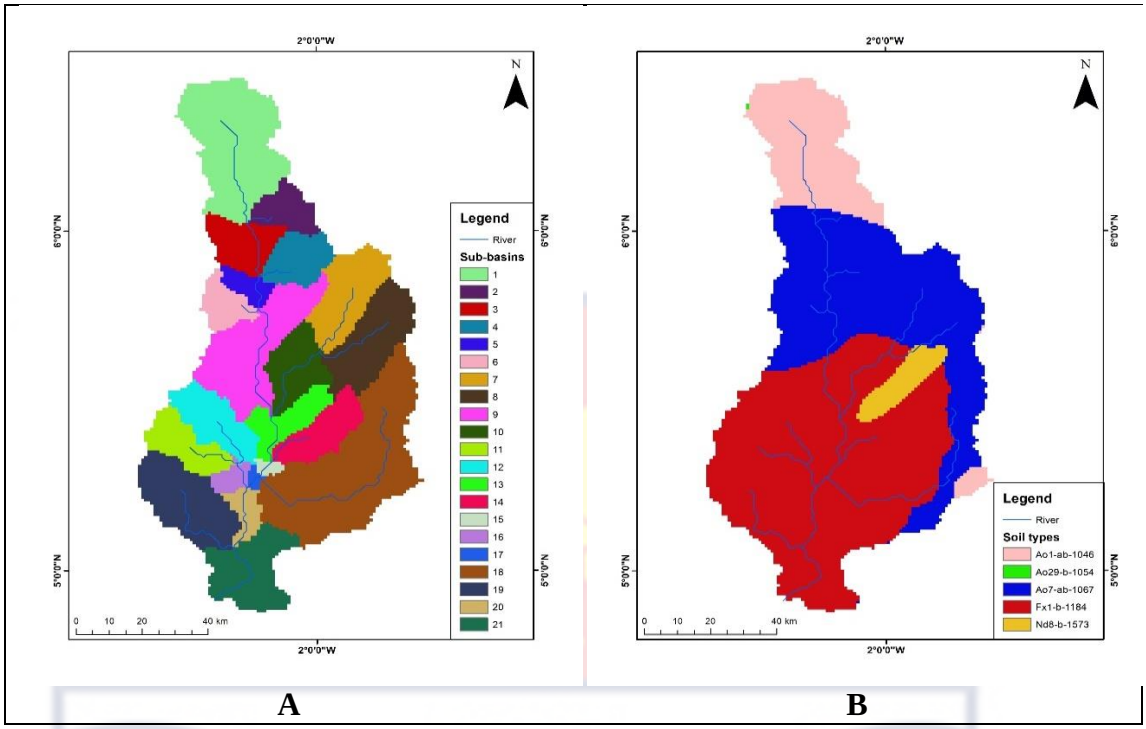

A **B**

Figure 14: SWAT outputs for the ARB- Sub-basins (A) and Soil types (B)

Source: Produced by the Researcher in SWAT

Table 19: Soil and slope characteristics in the ARB

Basin Parameter	Parameter characteristic	Area (km^2) covered by basin parameter	% of the total basin area
Soil	Ao1-ab-1046	1207.41	14.3
	Ao7-ab-1067	2877.84	34.0
	Fx1-b-1184	4124.68	48.8
	Nd8-b-1573	247.45	2.9
Slope	0-1%	7427.79	87.83
	>1%	1029.59	12.17

Source: Results of HRU analysis in SWAT model, produced and compiled by the Researcher

4.4.2 SWAT Calibration, validation and performance evaluation

Table 20 shows the evaluation statistics for the SWAT model. The model has NSE of 0.972 and PBIAs of -2.54 for calibration and NSE of 0.940 and PBIAs of 2.84 for validation. This implies an excellent model performance (Kenea et al., 2021) with a slight underestimation against

observed stream flow at calibration and overestimation at validation respectively. As can also be seen from Figures 15 and 16 which show results of model calibration and validation respectively, there is a strong agreement between the observed and simulated stream flow data. The model was therefore fit for estimating water yield from the basin.

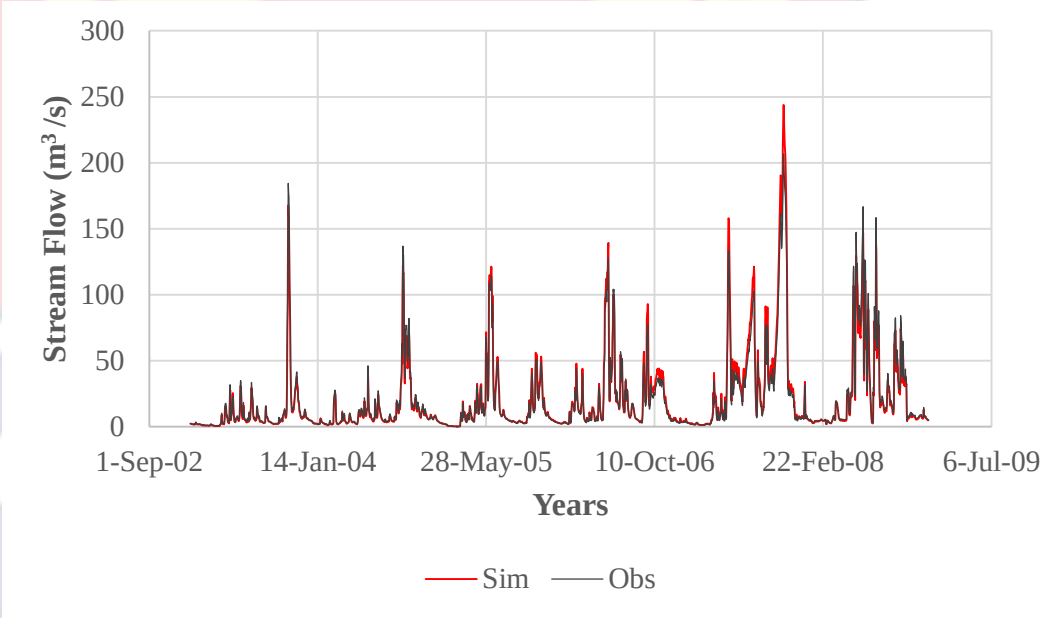

Figure 15: SWAT Model Calibration for the ARB

Source: Results of SWAT model calibration, produced by the Researcher

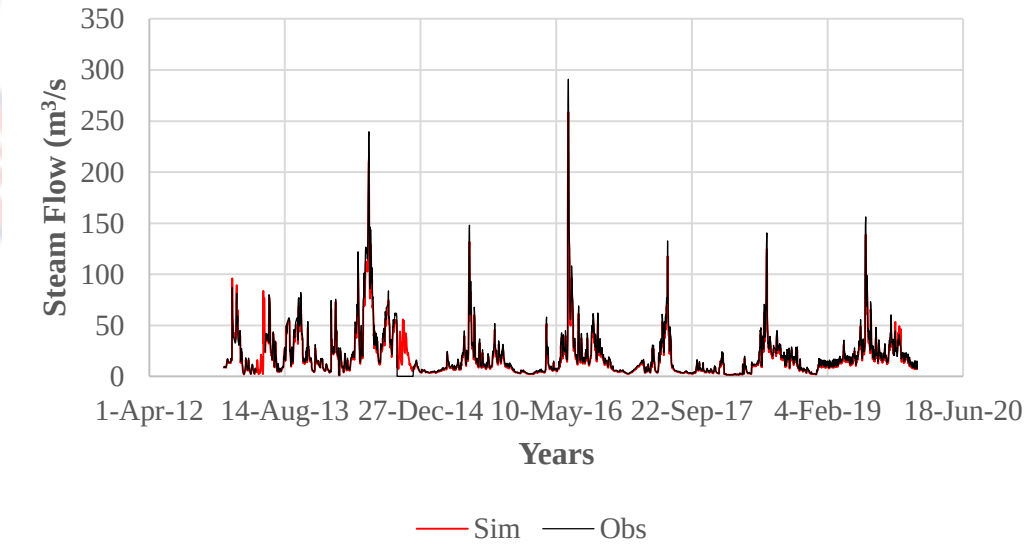

Figure 16: SWAT Model Validation for the ARB

Source: Results of SWAT model validation, produced by the Researcher

Table 20: SWAT model performance evaluation statistics

Model performance statistic	Calibration	Validation
NSE	0.972	0.940
PBIAS	-2.54	2.84

Source: Calculated by the Researcher in Microsoft Excel 2016 based on simulated and observed water yield output values from SWAT model.

4.4.3 Water yield generation

Water yield results were extracted from the SWAT output files. Table 21 shows summary of water yield from the ARB generated in 1991, 2008 and 2021, as hydrological response to the detected LULC changes in the years. Total annual yields were 355.64 mm, 494.91 mm and 481.55 mm respectively, with monthly peak yields of 101.11 mm recorded in July for 1991, 127.02 mm in August for 2008, and 113. 27 mm in October for 2021.

Table 21: Estimated water yield from the ARB

Month	Water yield in mm		
	1991	**2008**	**2021**
January	0.00	9.37	0.06
February	0.01	8.90	1.46
March	0.02	20.02	18.48
April	0.11	25.18	3.38
May	39.21	36.95	1.88
June	21.86	16.67	14.33
July	101.11	127.02	51.45
August	92.68	18.63	55.85
September	60.34	55.02	109.6
October	25.11	102.05	113.27
November	13.01	64.38	85.72
December	2.18	10.73	26.07
Total	**355.64**	**494.91**	**481.55**

Source: Compiled by the Researcher from SWAT model outputs

4.4.4 Correlation between water yield and land use and climatic factors in ARB

Table 22 is a summary of the status of the dominant land use land cover (dense vegetation, sparse vegetation and built-up/bare coverage), and climatic factors (rainfall and evaporation) as well as corresponding water yields in 1991, 2008 and 2021 in the ARB. It shows that in 1991, dense vegetation, sparse vegetation and built-up/bare coverage were 3844.5 km^2, 4365.0km^2 and 45 km^2 respectively. Total annual rainfall was 1088.51 mm while evaporation was 1000.5 mm. In 2008, dense vegetation, sparse vegetation and built-up/bare coverage were 2267.5 km^2, 5832.0 km^2 and 100.56 km^2 respectively, while total annual rainfall and evaporation where 1275.78 mm and 1031.4 mm respectively. In 2021, dense vegetation, sparse vegetation and built-up/bare land had an area coverage of 2267.5 km^2, 5832.0 km^2 and 100.56 km^2, respectively. Total annual rainfall was 2031.83 mm while evaporation was 1378.82 mm. The quantity of water in 1991, 2008 and 2021 were 355.64 mm, 494.91mm and 481.55 mm respectively.

The results therefore depict an increase in sparse vegetation and built-up/bare land area coverage, rainfall and evaporation, and a decrease in dense vegetation between 1991 and 2021 (Tabel 21). Within the same period water yield increased between 1991 and 2008 and decreased between 2008 and 2021.

Table 23 presents results of correlation analysis aimed at determining the association between the variables; land use land cover parametric, rainfall and evaporation. The result shows that there is strong negative correlation between water yield and dense vegetation, r = -0.983. This implies that as

dense vegetation decreases, water yield from the basin is expected to increase. However, the correction was not significant (p-value = 0.118) (Table 22). On the other hand, the study found a strong positive correlation between water yield sparse vegetation (r = 0.998). The correlation was significant (p-value = 0.0389). The study also found a moderate negative correlation between water yield and built-up/bare land (r = -0.526), which was also not significant (p-value = 0.648). The study also found an insignificant weak positive correlation between water yield and rainfall (r = 0.0488, p-value = 0.675).

Table 22: Variations in land use and hydro-climatic parameters

	Change		
Parameters	**1991**	**2008**	**2021**
Dense vegetation cover (km^2)	3844.5	2267.5	2075.97
Sparse vegetation cover (km^2)	4365.00	5832.00	5599.17
Built-up/bare land cover(km^2)	45.31	100.56	480.05
Total annual rainfall (mm)	1088.51	1275.78	2034.83
Total annual evaporation (mm)	1000.5	1031.4	1378.82
Total annual water yield (mm)	355.64	494.91	481.55

Source: Produced and compiled by the Researcher from land use change and hydrological analyses.

Table 23: Correlation among hydro-climatic parameters in the ARB

	WY	DV	SP	BB	Rn	Et
WY	1	r = -0.983 P-value = 0.118	**r = 0.998 P-value = 0.0389**	r = 0.526 P-value = 0.648	r = -0.585 P-value = 0.602	r = 0.0488 P-value = 0.675
DV		1	r = -0.970 P-value = 0.158	r = 0.674 P-value = 0.529	r = -0.725 P-value = 0.484	r = -0.641 P-value = 0.557
SP			1	r = 0.473 P-value = 0.687	r = 0.534 P-value = 0.641	r = 0.434 P-value = 0.714
BB				1	r = 0.997 P-value = 0.0453	**r = 0.999 P-value = 0.0275**
Rn					1	r = 0.993 P-value = 0.0728
Et						1

WY = Water yield; DV = Dense vegetation cover; SP = Sparse vegetation cover; BB = built-up / bare land cover; Rn = Rainfall; Et = Evaporation
Source: Produced and compiled by the Researcher based on land use change, hydrological and correlation analysis

4.4.5 Mapping of flood inundation in the ACA

Mapping was based on the peak water yield from the ARB for 1991, 2008 and 2021 to estimate the maximum potential extent of flood inundation from climate and LULC change impacts in the basin. Figure 17 shows flood inundation maps for 1991, 2008 and 2021, and superimposed overland on the vulnerability map for the ACA. Also, while Table 24 shows the inundation area coverage in each of the years. The areas at risk of flooding for 1991, 2008 and 2021 were 14.89 km^2, 23.50 km^2 and 18.31 km^2 respectively (Table 24). The results, therefore show that there was an increase in inundated area in the ACA linked to climatic and land use changes taking place in ARB between 1991 and 2021.

Table 24: Estimated inundated coastal area due to climate and LULC change in the ARB

Year	Area (km^2)	Communities at risk
1991	14.89	Sanwohma, Apa Taim and Adelekezo
2008	23.50	Sanwohma, Apa Taim and Adelekezo
2021	18.31	Sanwohma, Apa Taim and Adelekezo

Source: Compiled by the researcher based on water yield outputs from SWAT Model.

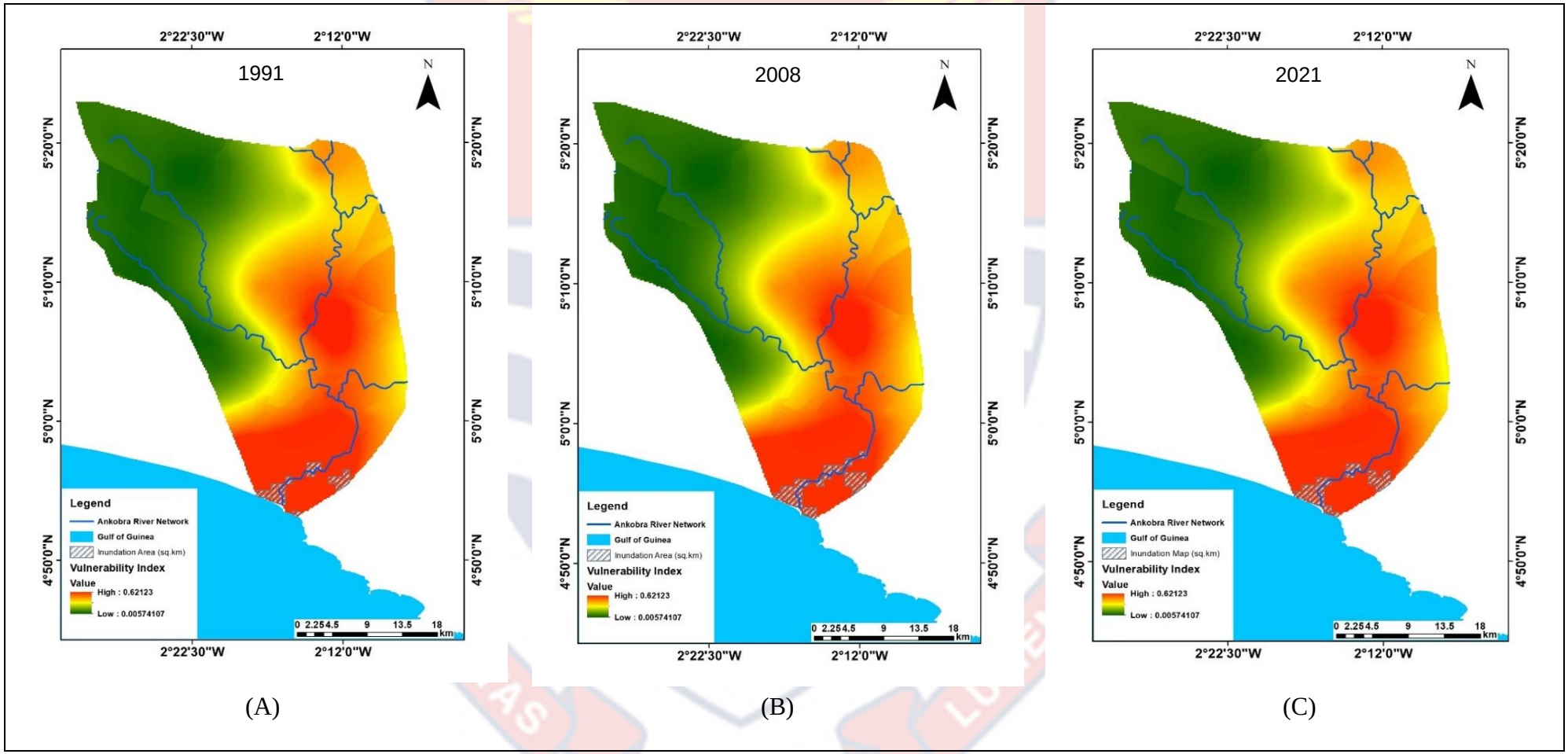

Figure 17: Coastal flood risk map due to climate and LULC change in the Ankobra River Basin

Source: Produced by the researcher in ArchMap based on yield generation from the ARB.

CHAPTER FIVE

DISCUSSIONS

5.1 Introduction

The purpose of this study was to assess the impact of climate and land use land cover change in the ARB on flood risk in the ACA in western Ghana. Specifically, it assessed changes in temperature, rainfall, and land use land cover in the basin. Further to this, it assessed the extent of inundation that could be attributed to the changes in the basin. Also, it characterised the vulnerability of coastal areas to the impacts of flood inundation to estimate flood risk. This chapter therefore discusses the results. Where possible, it makes reference to related studies to elucidate the findings. The chapter is structured under the main themes of the objectives of the study.

5.2 Land use land cover change in the Ankobra River Basin

From the findings, four land use classes dominate the ARB. These are water, built-up/bare land, dense vegetation, and cultivated/sparse vegetation (Figure 5). There were significant variations in land use observed over the period between 1991 and 2022. The period experienced a loss in dense vegetation cover by 1768. 5 km^2 representing 46 % (Table 11). The finding of this study agrees with that of Obodai, Adjei, Odai & Lumor (2019) who found a decrease in dense vegetation cover in the basin. In their study, Obodai *et al.* found out that dense vegetation covered 40.4 % and 22.8 % of the total basin area in different time periods compared to 30 % for this study. This minor difference could be due to classification algorithms and the method for calculating the change. The current study used maximum likelihood

classification algorithms compared to Spectral angle mapping that were used by Obodai et al. (2019).

Over the same period, the sum of land covered gain in water, built-up/bare land and cultivated/sparse coverage was equal to the land loss in dense vegetation (1787,56 km^2). The loss in the dense vegetation could therefore be explained by transformation of dense vegetation to other land uses, predominantly water, built-up/bare land and cultivated/sparse vegetation, and driven by anthropogenic activities. This agrees with the findings of Obodai et al. (2019) who also observed an increase in land covered by water due to small scale mining activities that are prevalent in the ARB, at the expense of vegetation. Small scale mining activities are associated with clearing of vegetation for other uses, rendering the land bare. In the process, river banks are also destabilized in the process, which causes water to spread beyond natural confinements of rivers. This is further confirmed by Awotwi, Anornu, Quaye-Ballard & Annor (2018), who found out that agriculture, mining and settlement were the main activities responsible for LULC change in the Pra River Basin (PRB) which shares boundaries with ARB.

5.3 Temperature and rainfall variations in Ankobra river basin

There are positive trends for both temperature and rainfall in the ACA. The increase in temperature is significant. The temperature trend in the basin is therefore no different from findings of other local, regional and global trends. A prediction study by Larbi et al. (2022) conducted in the Tano River Basin (TRB), which shares a boundary with the ARB predicted that the mean annual temperature would increase by 0.07 °C and 0.09 °C between 2021-2050, under RCP 4.5 and RCP 8.5 respectively. This study, however, found

that temperature increased by about 1 °C between 1986 and 2020. While the findings of the study agree with that of Larbi *et al.* on the positive trend, the difference the magnitude of change can be explained by the data that was used period covered in this study and that used by Larbi *et al.* The study used historic data observed between 1986 to 2020 (Table 12), while Larbi *et al.* predicted likely changes to in temperature to occur between 2021 to 2050 based on future assumptions under representative carbon concentration pathways.

The study further agrees with the results of a spatio-temporal assessment of temperature and rainfall in Ghana between 1900 and 2014 by Abbam et al. (2018) which also showed a significant increase in temperature across Ghana with the Western Region, where the study area falls, being one of the national hotspots. Furtherly, the study also agrees with global trends. Globally, the period between 2011 and 2020 was warmer by about 1.09°C relative to 1850-1900 (Zhou, 2021).

The increase in rainfall in the basin also agrees with related local studies but varies with regional and global findings. For example, Larbi et al. (2022) found out that the average annual rainfall of 1402 mm would rise by 0.5 % with a negative trend of 1.22 mm per year between 2021 and 2050 under the RCP4.5 scenario, to which this study's findings agree. Further to this, similar studies by Amisigo et al. (2018) indicated an increased projected water inflow into the Volta Lake due to increased projected annual rainfall in the Volta Basin under both the A1b and A2 SRES. Globally, it agrees with suggestions by Donat, Lowry, Alexander, O'Gorman & Maher (2016) that wet areas will get wetter, especially over oceans whose effects could spread to

coastal areas like parts of the ARB. It however varies with areas that do not share similar climatic conditions with the basin. For example, an analysis of rainfall between 1900 and 2014 by Abbam et al. (2018) showed that the northern regions of Ghana have become drier. As reported by IPCC (2021), global trends in precipitation are largely variable and are location specific. However, there is a general positive trend in the northern hemisphere and a negative trend in the southern hemisphere.

5.4 Impacts of variations in LULC, rainfall and temperature on water yield in Ankobra River Basin

Over the period between 1991 and 2021, the extent of land prone to flood inundation was estimated to range up to 23.5 km^2, observed in 2008. The extent of inundation has a strong positive association with change in extent of cultivated/sparse vegetation. It also has, although weak, a positive association with built-up/bare land and rainfall. This implies that the potential to flooding increases as rainfall, cultivated/sparse vegetation and built-up bare land increase. Such positive association was also observed in similar studies on the impacts of climate and land use land cover change on water balance at basin level in similar studies. For instance, in Ghana, Amisigo et al. (2018) found an increase in projected water inflow into the Volta Lake due to increased projected annual rainfall in the Volta Basin under both the A1b and A2 climate change scenarios. In West Africa, Nka et al. (2015) found a strongly significant association between flood and rainfall annual maxima in 11 watersheds in western Africa. In Ethiopia, an assessment of hydrological responses to LULC changes by Kenea et al. (2021) in the Fincha'a Watershed

in Ethiopia showed an increase in both wet and dry stream flow as a result of conversion of land coverage from forest and grass to build-up areas.

According to Wang et al. (2009) LULC change alters the dynamics of hydrological elements on land. Studies have further shown that changes in the characteristics of the land surface such as soil properties, surface roughness and vegetation properties, change the terrestrial hydrological system (Angeles et al.,2001). An increase in sparse vegetation of bare land in the Ankobra River Basin could therefore have resulted in increased runoff and hence water yield, which enhances potential for flood inundation from a particular rainfall event. The highest potential extent of flood inundation was observed in 2008, a period when the basin experienced the highest transformation of land use from dense vegetation to cultivated/sparse vegetation. This confirms the impacts of reduced vegetation cover on flood potential in the ACA. The increase in rainfall in the basin, though insignificant, would increase the potential to flooding mainly due to the influence of reduced vegetation cover in the basin.

5.5 Coastal Vulnerability and Flood Risk in the ACA due to Climate and LULC Changes in the ARB

5.5.1 Socio-economic and physical determinants of vulnerability in ACA

According to UNISDR (2009), vulnerability is defined as the 'characteristics and circumstances of a community, system or asset that make it susceptible to the damaging effects of a hazard'. According to Kontogianni et al. (2019), the characteristics are dependent on factors that define the sensitivity and adaptive capacity of a system.

In this study, socio-economic factors, including sex, age, education, income, access to productive natural resources, affiliation to social groups, and height of house foundations were assessed in the study area, to define its sensitivity and adaptive capacity to the impacts of floods. This is because, based on their magnitude, they may increase vulnerability by enhancing sensitivity or reduce adaptive capacity (Dolan & Walker, 2006; Hadipour et al., 2020; Marzi et al., 2019).

The findings of this study reveal that half (50.1%) of the household heads in the ACA attained only up to lower secondary level of education (less than 12 years of school attendance) (Table 14). The results slightly differ with the population census that was conducted in 2010 (Ghana Statistical Services 2013), which found out that the proportion of population that attained up to lower secondary level of education in the Western Region was 21.8 %. There seems to be an increase from 2010 to 2016, such that the higher proportion found in this study could be as a result of national efforts made in education service delivery over the period.

Furthermore, the study showed that the ACA is dominated by male headed households. Also, the majority (76%) of the household head fall in the range of 30 to 65 years. About 70% of the household heads in the ACA also do not belong to any formal social groupings. Lastly, most households (over 50%) have houses that have foundation of between 0.3m to 0.05 m. The combination of these socio-economic characteristics have complex impact on the level of vulnerability. For example, according to Cutter et al. (2003), male headed households easily recover from a disaster than their female counterpart, hence they tend to be less vulnerable than women headed

households. Also, extreme age spectrum reduces one's ability to resist damage but rather increases sensitivity to the impact of a hazard. For example, the elderly may have mobility limitations thereby increasing their vulnerability. Education also determines socio-economic status, such that higher education attainment results in greater lifetime earnings. Furthermore, lower education limits one's ability to comprehend and use risk information, including warning and response and recovery information. High and stable levels of income enable one to absorb and recover from losses more quickly. On the other hand, low income makes one incapable of adapting to disasters, while quality of residential construction affects potential losses and recovery. Mobile homes and those built from weak materials are easily destroyed and are less resilient to hazards. According to Marzi et al. (2019), affiliation to social groupings increase cohesion and social support in times of disasters as it increases one's ability to recover after a disaster event, while access to resources increases one's adaptive capacity.

Regarding physical variables that determine flood vulnerability in the ACA, this study considered elevation, distance to coastline, MWH and MTR as the major variables that measure coastal vulnerability as also used in the related studies along the coast of the Gulf of Guinea by Boateng et al. (2016); Evadzi et al. (2017) and Tano et al. (2018).

To understand the impacts of the various variables on the vulnerability of ACA to coastal flooding, normalisation and weighting of the both socio-economic and physical variables were done using Analytical Hierarchy Process (AHP). Income level and condition of the house of a household had the highest weights among socio-economic variables (Table 16). This implies

that income level and condition of the house of a household are the key socio-economic determinants of ACA to coastal flooding. Distance to coastline and elevation, on the other hand, had the highest weights among the physical variables, implying their strongest influence on the vulnerability of the coastal area to flooding. Sex and affiliation to social groupings were found to be the least influencing social variables, while MTR and MWH were the least influencing physical variables.

The findings agree with several similar studies that were conducted in the area. For example, Osman et al. (2016) found out that the top three factors that affect social vulnerability in Sanwohma are income, education, household conditions in terms of foundation and other building materials. For physical factors, Osman et al. (2016) also found distance to the coastline to be key to coastal vulnerability in the area.

Boateng et al. (2016) found out that vulnerability to SLR on the CoG is principally influenced by elevation and geology. The Nzema East district, where the study area is located, is precisely susceptible to flooding inundation from SLR due to low elevation and its sandy geological formation. Boateng *et al*. further found out that tidal range and wave height did not have significant role in determining the vulnerability of the area. Tano et al. (2018) found out that elevation is the most influencing factor on coastal vulnerability along the Ivorian coast, which shares boundaries with the western CoG.

5.5.2 Water yield and flood risk in the ACA

According to Reisinger et al. (2020), the expected impacts of a flood hazard on a systems, and the ability of the to respond determines floods risk. Flood risk is therefore, dependent on the characteristics of a hazard on one

hand, and vulnerability on the other hand (Bagewadi, 2017; Kang et al., 2018). In this study, flood inundation generated from the ARB in response to climate and LULC changes was regarded as the hazard due to its extrinsic nature to the ACA. While vulnerability is spread, with different levels across the ACA, flood risk between 1991 and 2021 was limited to not more than 23.5 km^2 (Table 24) The risk however, kept increasing over the years due to increase in water yield from the ARB, with a strong positive correlation to the transformation of dense vegetation to sparse vegetation or bare land. It is therefore, clear that changes in climatic conditions and land use land cover in the basin, which affect the amount of water yield from the basin had impacts on flood risk in the ACA.

This study was the first of its kind in the ARB and ACA. The findings, however, agreed with similar studies aimed at assessing the impacts of climate change and land use land cover changes in other basins. For example, Berihun et al. (2019) found out that a decrease in cultivated land at the expense of natural vegetation resulted in increased flood risk due to enhanced runoff from the upper blue Nile Basin in Ethiopia. In the same basin, while affirming the increased surface flow due to land cover modification from predominantly natural vegetation to predominantly cultivated and built-up land cover classes, Gashaw et al. (2018) further found that the changes resulted in reduced dry season, lateral and groundwater flows, as well as evapotranspiration. In Bangladesh, Adnan et al. (2020) found out that the construction of polders in the coastal region modified flood patterns, thus affirming the impact of LULC change on flood occurrences.

In the Gulf of Mexico, Brody et al. (2015) used statistical linear regression models to categorise the influence of different classes of LULC on losses due to floods. Their results showed significant reduction in the losses resulting from protecting some land classes, implying the importance of protecting some types of LULC in reducing floods in the coastal communities.

LULC influence flooding due to its influence on hydrological outputs such as annual flow, wet season flow, dry season flow, surface runoff, water yield, lateral flow, groundwater flow and evapotranspiration (Gashaw et al., 2018), and hence flood potential.

CHAPTER SIX

CONCLUSIONS AND RECOMMENDATIONS

The purpose of this study was to assess the impacts of climate and LULC change in the ARB on coastal flood risk in the ACA in western Ghana. To achieve this, four specific objectives were set. Objective 1 was to determine land use and land cover changes in the ARB between 1991 and 2022. In this regard, the study has shown that water, built-up/ bare land, and cultivated/sparse vegetation and dense vegetation dominate the basin. These LULC classes have undergone variations in coverage between 1991 and 2022. Over the period, dense vegetation has been reduced in the areas, which equals the sum of area gained by cultivated/sparse vegetation, built-up/bare land and water. As at 2022, sparse vegetation dominated the basin, and had a significant impact on flood risk in the ACA. Based on these findings, it is recommended that:

i. To reduce flood risk in the ACA, efforts should be made by the government of Ghana and other non-state organisation working in flood risk management to arrest transformation of dense vegetation to less dense land covers, such as sparse and bare land covers.

Objective 2 aimed at assessing climate variability in ARB using temperature and rainfall data between 1991 and 2021. In this regard, the study showed that temperature significantly increased in the basin. On the other hand, rainfall increased but not significantly. It is a common knowledge that increased temperature promotes evapotranspiration and changes in rainfall partners. On the other hand, increase in rainfall increases flood potential. It is therefore recommended that:

i. Further studies be continuously conducted in the basin to monitor for significant increases in rainfall on one hand, and to determine if increasing temperature in the ARB will lead to increased evaporation to the level of offsetting the water yield from the basin and reduced flood risk in the ACA.

Objective 3 was to assess the vulnerability of the ACA to coastal flooding based on physical and socio-economic factors. The study has shown that coastal flood in the ACA is mainly influenced by household income, conditions of houses, elevation and distance to coastline. Based on these factors, the study found out that the vulnerability is high in the southern section and decreases north-eastwards, and it is low in the north-western parts of the ACA. It is therefore recommended that:

i. Households that live in low-lying areas need to move to upper areas.
ii. Stakeholders in disaster risk management should introduce interventions that will improve income levels of people living in the ACA be enhanced.
iii. Households need to improve on the conditions of their houses, for example by adopting raised foundations and build with strong materials that can withstand any possible inundation.

Lastly, objective 4 was to estimate the extent of coastal flooding in the ACA from the effects of climate and LULC change in the ARB. The study found that the extent of potential flood inundation increased in the ACA principally with an increase in cultivated/sparse vegetation land use class in the ARB. Based on the findings, it is recommended that:

i. An integrated approach should be adopted to help flood risk management in the ACA. Flood risk management efforts should not only focus on the ACA but the entire ARB.

REFERENCES

Abass, K., Dumedah, G., Frempong, F., Muntaka, A. S., Appiah, D. O., Garsonu, E. K., & Gyasi, R. M. (2022). *Rising incidence and risks of floods in urban Ghana: Is climate change to blame?*. *Cities*, *121*, *103495*. https://doi.org/https://doi.org/10.1016/j.cities.2021.103495

Abbam, T., Johnson, F. A., Dash, J., & Padmadas, S. S. (2018). Spatiotemporal Variations in Rainfall and Temperature in Ghana Over the Twentieth Century, 1900–2014. *Earth and Space Science*, *5*(4), 120–132. https://doi.org/10.1002/2017EA000327

Abdi, H., & Williams, L. J. (2010). Principal component analysis. *Wiley Interdisciplinary Reviews: Computational Statistics*, *2*(4), 433–459. https://doi.org/10.1002/wics.101

Abrams, M., Crippen, R., & Fujisada, H. (2020). ASTER Global Digital Elevation Model (GDEM) and ASTER Global Water Body Dataset (ASTWBD). *Remote Sensing*, *12*(7), 1–12. https://doi.org/10.3390/rs12071156

Accastello, C., Cocuccioni, S., & Teich, M. (2016). The Concept of Risk and Natural Hazards. *Intech*, *11*(tourism), 13. https://www.intechopen.com/books/advanced-biometric-technologies/liveness-detection-in-biometrics

Adhikari, P., Hong, Y., Douglas, K. R., Kirschbaum, D. B., Gourley, J., Adler, R., & Brakenridge, G. R. (2010). A digitized global flood inventory (1998-2008): Compilation and preliminary results. *Natural Hazards*, *55*(2), 405–422. https://doi.org/10.1007/s11069-010-9537-2

Adnan, M. S. G., Abdullah, A. Y. M., Dewan, A., & Hall, J. W. (2020). The effects of changing land use and flood hazard on poverty in coastal Bangladesh. *Land Use Policy*, *99*, 1–29. https://doi.org/10.1016/j.landusepol.2020.104868

African Union Commission (2015). The African Union Commission: AGENDA 2063, The Africa We Want. First Ten-Year Implementation Plan. *African Union*, *April*, 201. https://au.int/en/agenda2063/overview%0Ahttps://au.int/sites/default/files/documents/36204-doc-agenda2063_popular_version_en.pdf%0Ahttp://www.un.org/en/africa/osaa/pdf/au/agenda2063.pdf

Ahadzie, D. K., Mensah, H., & Simpeh, E. (2022). Impact of floods, recovery, and repairs of residential structures in Ghana: insights from homeowners. *GeoJournal*, *87*(4), 3133-3148.

Ahsan, M. N., & Warner, J. (2014). The socioeconomic vulnerability index: A pragmatic approach for assessing climate change led risks-A case study in the south-western coastal Bangladesh. *International Journal of Disaster Risk Reduction*, *8*, 32–49. https://doi.org/10.1016/j.ijdrr.2013.12.009

Aman, A., Tano, R. A., Toualy, E., Silué, F., Addo, K. A., & Folorunsho, R. (2019). Physical Forcing Induced Coastal Vulnerability along the Gulf of Guinea. *Journal of Environmental Protection*, *10*(09), 1194–1211. https://doi.org/10.4236/jep.2019.109071

Amisigo, B. A., Logah, F. Y., & Obuobie, E. (2018). Impacts of Climate Change on Stream Inflows into the Volta Lake. *Ghana Journal of Science*, *58*(0), 23–33.

Anderson, J., Hardy, E., Roach, J., & Witmer, R. (1972). A Land Use Classification System for Use with Remote-Sensor Data; USGS Circular 671. *US Geological Survey: Washington, DC, USA*.

Angeles, L., Angeles, L., & Springs, C. (2001). *The Impact of Land Surface Processes on Simulations of the U . S . Hydrological Cycle : A Case Study of the 1993 Flood Using the SSiB Land Surface Model in the NCEP Eta Regional Model*. 2833–2860.

Appeaning-Addo, K. A., Larbi, L., Amisigo, B., & Ofori-Danson, P. K. (2011). Impacts of coastal inundation due to climate change in a cluster of urban coastal communities in Ghana, West Africa. *Remote Sensing*, *3*(9), 2029–2050. https://doi.org/10.3390/rs3092029

Appeaning Addo, K., Jayson-Quashigah, P. N., Codjoe, S. N. A., & Martey, F. (2018). Drone as a tool for coastal flood monitoring in the Volta Delta, Ghana. *Geoenvironmental Disasters*, *5*(1). https://doi.org/10.1186/s40677-018-0108-2

Arnous, M. O., & Green, D. R. (2011). GIS and remote sensing as tools for conducting geo-hazards risk assessment along Gulf of Aqaba coastal zone, Egypt. *Journal of Coastal Conservation*, *15*, 457-475.

Arrieta-Castro, M., Donado-Rodríguez, A., Acuña, G. J., Canales, F. A., Teegavarapu, R. S. V., & Kaźmierczak, B. (2020). Analysis of streamflow variability and trends in the meta river, Colombia. *Water (Switzerland)*, *12*(5). https://doi.org/10.3390/w12051451

Asumadu-Sarkodie, S., Owusu, P. A., & Rufangura, P. (2017). Impact analysis of flood in Accra, Ghana.

Awotwi, A., Anornu, G. K., Quaye-Ballard, J. A., & Annor, T. (2018). Monitoring land use and land cover changes due to extensive gold mining, urban expansion, and agriculture in the Pra River Basin of Ghana, 1986–2025. *Land Degradation and Development*, *29*(10), 3331–3343. https://doi.org/10.1002/ldr.3093

Bagewadi, P. (2017). *Calculating Disaster Risk Index (DRI) for Greater Mumbai by Hazard Risk and Vulnerability Analysis (HRVA) using GIS*. *4*(10), 101–107.

Baldassarre, G. Di, Montanari, A., Lins, H., Koutsoyiannis, D., Brandimarte, L., & Blöschl, G. (2010). *Flood fatalities in Africa : From diagnosis to mitigation*. *37*(September), 2–6. https://doi.org/10.1029/2010GL045467

Bhattacharya, T., & Guleria, S. (2012). Coastal flood management in rural planning unit through land-use planning: Kaikhali, West Bengal, India. *Journal of Coastal Conservation*, *16*(1), 77-87

Berihun, M. L., Tsunekawa, A., Haregeweyn, N., Meshesha, D. T., Adgo, E., Tsubo, M., Masunaga, T., Fenta, A. A., Sultan, D., Yibeltal, M., & Ebabu, K. (2019). Hydrological responses to land use/land cover change and climate variability in contrasting agro-ecological environments of the Upper Blue Nile basin, Ethiopia. *Science of the Total Environment*, *689*, 347–365. https://doi.org/10.1016/j.scitotenv.2019.06.338

Boateng, I., Wiafe, G., & Jayson-Quashigah, P. N. (2016). Mapping Vulnerability and Risk of Ghana's Coastline to SLR. *Marine Geodesy*, *40*(1), 23–39. https://doi.org/10.1080/01490419.2016.1261745

Brath, A., Montanari, A., & Moretti, G. (2006). Assessing the effect on flood frequency of land use change via hydrological simulation (with uncertainty). *Journal of Hydrology*, *324*(1–4), 141–153. https://doi.org/10.1016/j.jhydrol.2005.10.001

Brody, S. D., Highfield, W. E., & Blessing, R. (2015). An Analysis of the Effects of Land Use and Land Cover on Flood Losses along the Gulf of Mexico Coast from 1999 to 2009. *Journal of the American Water Resources Association*, *51*(6), 1556–1567. https://doi.org/10.1111/1752-1688.12331

Cudjoe, S., & Kwabla Alorvor, S. (2021). Indigenous Knowledge Practices and Community Adaptation to Coastal Flooding in Ada East District of Ghana. *Hydrology*, *9*(1), 13. https://doi.org/10.11648/j.hyd.20210901.12

Cutter, S. L., Boruff, B. J., & Shirley, W. L. (2003). Social vulnerability to environmental hazards. *Social Science Quarterly*, *84*(2), 242–261. https://doi.org/10.1111/1540-6237.8402002

Daly, E., Calabrese, S., Yin, J., & Porporato, A. (2019). Hydrological spaces of long-term catchment water balance. *Water Resources Research*, *55*(12), 10747-10764.

Dasgupta, S., & Meisner, C. (2009a). Climate Change and SLR A Review of the Scientific Evidence Climate Change. *The World Bank Environment Department*, *118*, 118.

Dasgupta, S., & Meisner, C. (2009b). Climate Change and SLR A Review of the Scientific Evidence Climate Change. *The World Bank Environment Department*, *118*, 118.

Demir, V., & Kisi, O. (2016). *Flood Hazard Mapping by Using Geographic Information System and Hydraulic Model : Mert River , Samsun , Turkey*. *2016*.

Dolan, A. H., & Walker, I. J. (2006). Understanding vulnerability of coastal communities to climate change related risks. *Journal of Coastal research*, 1316-1323.Donat, M. G., Lowry, A. L., Alexander, L. V., O'Gorman, P. A., & Maher, N. (2016). More extreme precipitation in the worldâ €TM s dry and wet regions. *Nature Climate Change*, *6*(5), 508–513. https://doi.org/10. 1038/nclimate2941

Douglas, I., Alam, K., Maghenda, M., Mcdonnell, Y., Mclean, L., & Campbell, J. (2008). Unjust waters: Climate change, flooding and the urban poor in Africa. *Environment and Urbanization*, *20*(1), 187–205. https://doi.org/10.1177/0956247808089156

Espina, N. B. (2018). Planning for Climate Resilient Barangays in the Philippines: The Case of Barangay Tumana in Marikina City, Metro Manila. *Consilience: The Journal of Sustainable Development*, *19*(1), 130–162.

Evadzi, P. I. K., Zorita, E., & Hünicke, B. (2017). Quantifying and Predicting the Contribution of SLR to Shoreline Change in Ghana: Information for Coastal Adaptation Strategies. *Journal of Coastal Research*, *33*(6), 1283–1291. https://doi.org/10.2112/JCOASTRES-D-16-00119.1

Fekete, A. (2009). Validation of a social vulnerability index in context to river-floods in Germany. *Natural Hazards and Earth System Science*, *9*(2), 393–403. https://doi.org/10.5194/nhess-9-393-2009

Field, C. B. (Ed.). (2012). *Managing the risks of extreme events and disasters to advance climate change adaptation: special report of the intergovernmental panel on climate change*. Cambridge University Press.

Fox-Kemper, B., Hewitt, H. T., Xiao, C., Aðalgeirsdóttir, G., Drijfhout, S. S., Edwards, T. L., ... & Krinner, G. others. 2021. Ocean, cryosphere and sea level change. Chapter 9 in Climate Change 2021: *The Physical Science Basis. Contribution of Working Group I to the Sixth Assessment Report of the Intergovernmental Panel on Climate Change*. Cambridge University Press.

Füssel, H. M. (2007). Vulnerability: A generally applicable conceptual framework for climate change research. *Global Environmental Change*, *17*(2), 155–167. https://doi.org/10.1016/j.gloenvcha.2006.05.002

Gashaw, T., Tulu, T., Argaw, M., & Worqlul, A. W. (2018). Modeling the hydrological impacts of land use/land cover changes in the Andassa watershed, Blue Nile Basin, Ethiopia. *Science of the Total Environment, 619–620,* 1394–1408. https://doi.org/10.1016/j.scitotenv.2017.11.191

Gaume, E., Bain, V., Bernardara, P., Newinger, O., Barbuc, M., Bateman, A., Blaškovičová, L., Blöschl, G., Borga, M., Dumitrescu, A., Daliakopoulos, I., Garcia, J., Irimescu, A., Kohnova, S., Koutroulis,

A., Marchi, L., Matreata, S., Medina, V., Preciso, E., … Viglione, A. (2009). A compilation of data on European flash floods. *Journal of Hydrology*, *367*(1–2), 70–78. https://doi.org/10.1 016/j.jhydrol.2008. 12.028

Ge, Y., Dou, W., & Liu, N. (2017). Planning resilient and sustainable cities: Identifying and targeting social vulnerability to climate change. *Sustainability (Switzerland)*, *9*(8). https://doi.org/10.3390/su9081394

Gevana, D., Camacho, L., Carandang, A., Camacho, S., & Im, S. (2015). Land use characterization and change detection of a small mangrove area in Banacon Island, Bohol, Philippines using a maximum likelihood classification method. *Forest Science and Technology*, *11*(4), 197–205. https://doi.org/10.1080/21580103.2014.996611

Ghana Statistical Services. (2013). *Population & housing census*.

Gladilshchikova, A. A., & Semenov, S. M. (2017). the Intergovernmental Panel on Climate Change (Ipcc): the Cycle of the Sixth Assessment Report. *Fundamental and Applied Climatology*, *2*(August 2021), 13–25. https://doi.org/10.21513/2410-8758-2017-2-13-25

Godschalk, D. R., & Burns, C. J. (2019). Coastal zone management. *Encyclopedia of Ocean Sciences*, 500–506. https://doi.org/10.1016 /B978-0-12-409548-9.11378-8

Gornitz, V. M., Daniels, R. C., White, T. W., & Birdwell, K. R. (1994). The Development of a Coastal Risk Assessment Database: Vulnerability to SLR in the U.S. Southeast. *Coastal and Estuarine Research Federation*, *12*, 327–338.

Hadi, S. J., Shafri, H. Z. M., & Mahir, M. D. (2014). Modelling LULC for the period 2010-2030 using GIS and remote sensing: A case study of Tikrit, Iraq. *IOP Conference Series: Earth and Environmental Science*, *20*(1). https://doi.org/10.1088/1755-1315/20/1/012053

Hadipour, V., Vafaie, F., & Deilami, K. (2020). *Coastal Flooding Risk Assessment Using a GIS-Based Spatial Multi-Criteria Decision Analysis Approach*.

Halim B. A., & Hasnita B. H. (2017). Determining Sample Size for Research Activities : The Case of Organizational Research. *Selangor Business Review*, *2*(1), 20–34.

Hayhoe, K., Edmonds, J., Kopp, R. E., LeGrande, A. N., Sanderson, B. M., Wehner, M. F., & Wuebbles, .J. (2017). Climate models, scenarios, and projections. *Climate Science Special Report: Fourth National Climate Assessment, I*, 133–160. https://doi.org/10.7930/J0WH2N54.U.S.

Hinkel, J., Lincke, D., Vafeidis, A. T., Perrette, M., Nicholls, R. J., Tol, R. S. J., Marzeion, B., Fettweis, X., Ionescu, C., & Levermann, A. (2014). Coastal flood damage and adaptation costs under 21st century SLR. *Proceedings of the National Academy of Sciences of the United States of America*, *111*(9), 3292–3297. https://doi.org/10.1073/pnas.1222469111

Hirsch, R. M., Slack, J. R., & Geological, U. S. (1984). A Nonparametric Trend Test for Seasonal Data With Serial Dependence. *Water Resources*, *20*(6), 727–732.

Huntington, T. G. (2006). Evidence for intensification of the global water cycle: Review and synthesis. *Journal of Hydrology*, *319*(1–4), 83–95. https://doi.org/10.1016/j.jhydrol.2005.07.003

Hussein, K., Alkaabi, K., Ghebreyesus, D., Liaqat, M. U., & Sharif, H. O. (2020). Land use/land cover change along the Eastern Coast of the UAE and its impact on flooding risk. *Geomatics, Natural Hazards and Risk*, *11*(1), 112–130. https://doi.org/10.1080/19475705.2019.1707718

IPCC. (2021a). Chp. 12: Climate change information for regional impact and for risk assessment. *Ipcc Ar6*, *August 2021*, 351–364.

IPCC. (2021b). Future Global Climate: Scenario-Based Projections and Near-Term Information. *Climate Change 2021: The Physical Science Basis. Contribution of Working Group I to the Sixth Assessment Report of the Intergovernmental Panel on Climate Change*, *August*, 195. https://www.ipcc.ch/report/ar6/wg1/#FullReport

Jevrejeva, S., Palanisamy, H., & Jackson, L. P. (2020). Global mean thermosteric sea level projections by 2100 in CMIP6 climate models. *Environmental Research Letters*, *16*(1). https://doi.org/10.1088/1748-9326/abceea

Jury, M. R., & Lucio, F. D. E. (2004). The Mozambique floods of February 2000 in context. *South African Geographical Journal*, *86*(2), 141-146.

Kang, T. S., Oh, H. M., Lee, E. Il, & Jeong, K. Y. (2018). Disaster Vulnerability Assessment in Coastal Areas of Korea. *Journal of Coastal Research*, *85*(85), 886–890. https://doi.org/10.2112/SI85-178.1

Karley, N. K. (2016). Floodind and physical planning in urban areas in west Africa: Situational Analysis of Accra, Ghana. *Https://Medium.Com/*, *4*(4), 25–41. https://doi.org/https://www.jstor.org/stable/10.2307/24872616

Katsman, C. A., Hazeleger, W., Drijfhout, S. S., Van Oldenborgh, G. J., & Burgers, G. (2008). Climate scenarios of SLR for the northeast Atlantic Ocean: A study including the effects of ocean dynamics and gravity changes induced by ice melt. *Climatic Change*, *91*(3–4), 351–374. https://doi.org/10.1007/s10584-008-9442-9

Kenea, U., Adeba, D., Regasa, M. S., & Nones, M. (2021). Hydrological responses to land use land cover changes in the fincha'a watershed, Ethiopia. *Land*, *10*(9). https://doi.org/10.3390/land10090916

Kim, J. E. J. Y. J.-H. T.-W. (2019). Socioeconomic vulnerability assessment of drought using principal component analysis and entropy method. *Journal of Korea Water Resources Association*, *52*(6), 441–449. https://doi.org/10.3741/JKWRA.2019.52.6.441

Kim, J. E., Yu, J., Ryu, J. H., Lee, J. H., & Kim, T. W. (2021). Assessment of regional drought vulnerability and risk using principal component analysis and a Gaussian mixture model. *Natural Hazards*, *109*(1), 707–724. https://doi.org/10.1007/s11069-021-04854-y

Kindu, M., Schneider, T., Teketay, D., & Knoke, T. (2013). Land use/land cover change analysis using object-based classification approach in Munessa-Shashemene landscape of the Ethiopian highlands. *Remote sensing*, *5*(5), 2411-2435.

Koks, E. E., Jongman, B., Husby, T. G., & Botzen, W. J. W. (2015). Combining hazard, exposure and social vulnerability to provide lessons for flood risk management. *Environmental Science and Policy*, *47*, 42–52. https://doi.org/10.1016/j.envsci.2014.10.013

Kontogianni, A., Damigos, D., Kyrtzoglou, T., Tourkolias, C., & Skourtos, M. (2019). Development of a composite climate change vulnerability index for small craft harbours. *Environmental Hazards*, *18*(2), 173–190. https://doi.org/10.1080/17477891.2018.1512469

Kumar, M., Kalra, N., Singh, H., Sharma, S., Rawat, P. S., Singh, R. K., ... & Ravindranath, N. H. (2021). Indicator-based vulnerability assessment of forest ecosystem in the Indian Western Himalayas: An analytical hierarchy process integrated approach. *Ecological Indicators*, *125*, 107568.

Larbi, I., Nyamekye, C., Dotse, S. Q., Danso, D. K., Annor, T., Bessah, E., Limantol, A. M., Attah-Darkwa, T., Kwawuvi, D., & Yomo, M. (2022). Rainfall and temperature projections and the implications on streamflow and evapotranspiration in the near future at the Tano River Basin of Ghana. *Scientific African*, *15*, e01071. https://doi.org/10.1016/j.sciaf. 2021.e01071

Liu, J., & Niyogi, D. (2019). Meta-analysis of urbanization impact on rainfall modification. *Scientific Reports*, *9*(1), 1–14. https://doi.org/10.1038/s41598-019-42494-2

Loster, T. (1999, June). Flood trends and global change. In *Proceedings IIASA Conf on Global Change and Catastrophe Management: Flood Risks in Europe*.Lu, H., Yan, Y., Zhu, J., Jin, T., Liu, G., Wu, G., ... &

Dallimer, M. (2020). Spatiotemporal water yield variations and influencing factors in the Lhasa River Basin, Tibetan Plateau. *Water*, *12*(5), 1498.

Lyu, K., Zhang, X., & Church, J. A. (2020). Regional Dynamic Sea Level Simulated in the CMIP5 and CMIP6 Models: Mean Biases, Future Projections, and Their Linkages. *Journal of Climate*, *33*(15), 6377–6398. https://doi.org/10.1175/JCLI-D-19-1029.1

Maanan, M., Maanan, M., Rueff, H., Adouk, N., Zourarah, B., & Rhinane, H. (2018). Assess the human and environmental vulnerability for coastal hazard by using a multi-criteria decision analysis. *Human and* 10807039.2017.1421452

Marchi, L., Borga, M., Preciso, E., & Gaume, E. (2010). Characterisation of selected extreme flash floods in Europe and implications for flood risk management. *Journal of Hydrology*. https://doi.org/doi:10.1016/j.jhydrol.2010.07.017

Marzi, S., Mysiak, J., Essenfelder, A. H., Amadio, M., Giove, S., & Fekete, A. (2019). Constructing a comprehensive disaster resilience index: The case of Italy. *PLoS ONE*, *14*(9), 1–23. https://doi.org/ 10.1371/ journal.pone.0221585

Merz, B., Kreibich, H., Schwarze, R., & Thieken, A. (2010). Review article "assessment of economic flood damage." *Natural Hazards and Earth System Science*, *10*(8), 1697–1724. https://doi.org/10.5194/nhess-10-1697-2010

Mimura, N. (2013). SLR caused by climate change and its implications for society. *Proceedings of the Japan Academy Series B: Physical and Biological Sciences*, *89*(7), 281–301. https://doi.org/10.2183/pjab.89.281

Naing, N. N. (2003). Determination of sample size. *Malaysian Journal of Medical Sciences*, *10*(2), 84–86.

Najibi, N., & Devineni, N. (2018). *Recent trends in the frequency and duration of global floods*. 757–783.

Nka, B. N., Oudin, L., Karambiri, H., Paturel, J. E., & Ribstein, P. (2015). Trends in floods in West Africa: Analysis based on 11 catchments in the region. *Hydrology and Earth System Sciences*, *19*(11), 4707–4719. https://doi.org/10.5194/hess-19-4707-2015

Obodai, J., Adjei, K. A., Odai, S. N., & Lumor, M. (2019). Land use/land cover dynamics using landsat data in a gold mining basin-the Ankobra, Ghana. In *Remote Sensing Applications: Society and Environment* (Vol. 13). Elsevier B.V. https://doi.org/10.1016/j.rsase.2018.10.007

Osei, M. A., Amekudzi, L. K., Omari-Sasu, A. Y., Yamba, E. I., Quansah, E., Aryee, J. N. A., & Preko, K. (2021). Estimation of the return periods of maxima rainfall and floods at the Pra River Catchment, Ghana, West Africa using the Gumbel extreme value theory. *Heliyon*, *7*(5), e06980. https://doi.org/10.1016/j.heliyon.2021.e06980

Osman, A., Ko, B., & Mariwah, S. (2016). *International Journal of Disaster Risk Reduction Vulnerability and risk levels of communities within Ankobra estuary of Ghana*. *19*, 133–144. https://doi.org/10.1016/j.ijdrr.2016.08.016

Osman, A., Nyarko, B. K., & Mariwah, S. (2016). Vulnerability and risk levels of communities within Ankobra estuary of Ghana. *International Journal of Disaster Risk Reduction*, *19*, 133–144. https://doi.org/10.1016/j.ijdrr.2016.08.016

Owusu, P. A., Asumadu-Sarkodie, S., & Ameyo, P. (2016). A review of Ghana's water resource management and the future prospect. *Cogent Engineering*, *3*(1). https://doi.org/10.1080/23311916.2016.1164275

Pachemska, T. A.-, Lapevski, M., & Timovski, R. (2014). Analytical Hierarchical Process (AHP) method application in the process of selection and evaluation. *Proceedings. Gabrovo: Internatinal Scientific Conference "UNITECH". 21-22 November 2014, November*, 373–380. https://www.researchgate.net/publication/276985609.

Park, S. J., & Lee, D. K. (2020). Prediction of coastal flooding risk under climate change impacts in South Korea using machine learning algorithms. *Environmental Research Letters*, *15*(9). https://doi.org/10.1088/1748-9326/aba5b3

Patel, K., Jain, R., Patel, A. N., & Kalubarme, M. H. (2021). Shoreline change monitoring for coastal zone management using multi-temporal Landsat data in Mahi River estuary, Gujarat State. *Applied Geomatics*, *13*, 333-347.

Phongsapan, K., Chishtie, F., Poortinga, A., Bhandari, B., Meechaiya, C., Kunlamai, T., Aung, K. S., Saah, D., Anderson, E., Markert, K., Markert, A., & Towashiraporn, P. (2019). Operational Flood Risk Index Mapping for Disaster Risk Reduction Using Earth Observations and Cloud Computing Technologies: A Case Study on Myanmar.

Frontiers in Environmental Science, *7*(December), 1–15. https://doi. org/1 0.3389/fenvs.2019.00191

Pour, S. H., Abd Wahab, A. K., Shahid, S., Asaduzzaman, M., & Dewan, A. (2020). Low impact development techniques to mitigate the impacts of climate-change-induced urban floods: Current trends, issues and challenges. *Sustainable Cities and Society*, https://doi.org/https://doi. org/10.1016 /j.scs.2020.102373

Prastica, R. M. S., & Fanani, A. J. (2021). What causes Ngancar River in Wiroko Temon sub-watershed vulnerable to flooding? *IOP Conference Series: Earth and Environmental Science*, *847*(1). https://doi.org/ 10.1088/1755-1315/847/1/012003

Reisinger, A., Howden, M., Vera, C., Garschagen, M., Hurlbert, M., Kreibiehl, S., Mach, K. J., Mintenbeck, K., O'neill, B., Pathak, M., Pedace, R., Pörtner, H.-O., Poloczanska, E., Rojas Corradi, M., Sillmann, J., Van Aalst, M., Viner, D., Jones, R., Ruane, A. C., & Ranasinghe, R. (2020). The concept of risk in the IPCC Sixth Assessment Report: a summary of cross-working group discussions. *Intergovernmental Panel on Climate Change, Geneva, Switzerland. Pp15, September*, 15.

Ribot, J. C. (1995). The causal structure of vulnerability: Its application to climate impact analysis. *GeoJournal*, 119-122.Roberts, C. M., Bohnsack, J. A., Gell, F., Hawkins, J. P., & Goodridge, R. (2001). Effects of marine reserves on adjacent fisheries. *Science*, *294*(5548), 1920–1923. https://doi.org/10.1126/science.294.5548.1920

Rocha, C., Antunes, C., & Catita, C. (2020). Coastal vulnerability assessment due to SLR: The case study of the Atlantic coast of Mainland Portugal. *Water (Switzerland)*, *12*(2). https://doi.org/10.3390/w12020360

Rwanga, S. S., & Ndambuki, J. M. (2017). Accuracy Assessment of Land Use/Land Cover Classification Using Remote Sensing and GIS. *International Journal of Geosciences*, *08*(04), 611–622. https://doi.org/10.4236/ijg.2017.84033

Saaty, T. L. (1977). *A scaling Methind for Priorities in Hierarchical Structures*. *281*, 234–281. https://doi.org/https://doi.org/10.1016/0022-2496(77)90033-5

Saghafian, B., Farazjoo, H., Bozorgy, B., & Yazdandoost, F. (2008). Flood intensification due to changes in land use. *Water Resources Management*, *22*(8), 1051–1067. https://doi.org/10.1007/s11269-007-9210-z

Sagoe-Addy, K., & Appeaning Addo, K. (2013). Effect of predicted sea level rise on tourism facilities along Ghana's Accra coast. *Journal of coastal conservation*, *17*(1), 155-166.

Schulze, R. E. (2000). Modelling hydrological responses to land use and climate change: a southern African perspective. *Ambio*, 12-22.

Sharif, H. O., Al-Juaidi, F. H., Al-Othman, A., Al-Dousary, I., Fadda, E., Jamal-Uddeen, S., & Elhassan, A. (2016). Flood hazards in an urbanizing watershed in Riyadh, Saudi Arabia. *Geomatics, Natural Hazards and Risk*, *7*(2), 702–720. https://doi.org/10.1080/19475705.2014.945101

Sheng, J., & Wilson, J. P. (2009). Watershed urbanization and changing flood behavior across the Los Angeles metropolitan region. *Natural Hazards*, *48*(1), 41–57. https://doi.org/10.1007/s11069-008-9241-7

Syvitski, J. P. M., & Robert Brakenridge, G. (2013). Causation and avoidance of catastrophic flooding along the Indus River, Pakistan. *GSA Today*, *23*(1), 4–10. https://doi.org/10.1130/GSATG165A.1

Tano, R. A., Aman, A., Toualy, E., Kouadio, Y. K., François-Xavier, B. B. D., & Addo, K. A. (2018). Development of an Integrated Coastal Vulnerability Index for the Ivorian Coast in West Africa. *Journal of Environmental Protection*, *09*(11), 1171–1184. https://doi.org/10.4236/jep.2018.911073

Tanoue, M., Hirabayashi, Y., & Ikeuchi, H. (2016). Global-scale river flood vulnerability in the last 50 years. *Scientific Reports*, *6*, 1–9. https://doi.org/10.1038/srep36021

Tompkins, E., & Mileti, D. (2005). Climate change vulnerability assessments: An evolution of conceptual thinking. *CLIM*.

Ullah, F., Saqib, S. E., Ahmad, M. M., & Fadlallah, M. A. (2020). Flood risk perception and its determinants among rural households in two communities in Khyber Pakhtunkhwa, Pakistan. *Natural Hazards*, *104*, 225-247.

UNISDR. (2009). *Terminilogies on Disaster Risk Reduction*.

UNISDR. (2015). Sendai Framework for Disaster Risk Reduction 2015-2030. *United Nations*. www.preventionweb.net/go/sfdrr

Vitousek, S., Barnard, P. L., Fletcher, C. H., Frazer, N., Erikson, L., & Storlazzi, C. D. (2017). Doubling of coastal flooding frequency within decades due to SLR. *Scientific Reports*, *7*(1), 1–9. https://doi.org /10.1038/s41598-017-01362-7

Wang, G., Xia, J., & Che, J. (2009). Quantification of effects of climate variations and human activities on runoff by a monthly water balance model: A case study of the Chaobai River basin in northern China. *Water Resources Research*, *45*(7), 1–12. https://doi.org/10.1029/2007 WR00 6768

Wasko, C. (2021). *Can temperature be used to inform changes to flood extremes with global warming?. Philosophical Transactions of the Royal Society A, 379(2195), 20190551.* https://doi.org/https://doi. org/10.1098/rsta.2019.0551

Wu, C. C., Jhan, H. T., Ting, K. H., Tsai, H. C., Lee, M. T., Hsu, T. W., & Liu, W. H. (2016). Application of social vulnerability indicators to climate change for the southwest coastal areas of Taiwan. *Sustainability (Switzerland)*, *8*(12). https://doi.org/10.3390/su8121270

Xuan Do, H., Zhao, F., Westra, S., Leonard, M., Gudmundsson, L., Eric Stanislas Boulange, J., Chang, J., Ciais, P., Gerten, D., Gosling, S. N., Müller Schmied, H., Stacke, T., Telteu, C. E., & Wada, Y. (2020). Historical and future changes in global flood magnitude - evidence from a model-observation investigation. *Hydrology and Earth System Sciences*, *24*(3), 1543–1564. https://doi.org/10.5194/hess-24-1543-2020

Yang, P., Wang, W., Xia, J., Chen, Y., Zhan, C., Zhang, S., Wei, C., Luo, X., & Li, J. (2022). Effects of climate change on major elements of the hydrological cycle in Aksu River basin, northwest China. *International Journal of Climatology*, *42*(10), 5359–5372. https://doi.org/10.1002/joc.7537

Zhou, T. (2021). New physical science behind climate change: What does IPCC AR6 tell us? *The Innovation*, *2*(4), 100173. https://doi.org/10.1016/j.xinn.2021.100173

Zou, L., & Thomalla, F. (2010). Social vulnerability to coastal hazards in South-east Asia: a synthesis of research insights. *Tropical deltas and coastal zones: Food production, communities and environment at the land and water interface*, 367-383.

APPENDICES

Appendix 1: Error Matrix for LULC Change in ARB

Land Use Class	Water	Developed/ Bare Land	Dense Vegetation	Cultivated/ Sparse Vegetation	Total (User)
Water	**6**	0	0	2	**8**
Developed/Bare Land	0	**9**	1	0	**10**
Dense Vegetation	0	0	**5**	0	**5**
Cultivated/Sparse Vegetation	1	0	0	**6**	**7**
Total (Producer)	**7**	**9**	**6**	**8**	**30**

Source: Produced and compiled by the Researcher

Appendix 2: Kappa Statistics

Land Use Class	User Accuracy (%)	Producer Accuracy (%)
Water	75	86
Developed/Bare Land	90	100
Dense Vegetation	100	83
Cultivated/Sparse Vegetation	86	75

Overall Accuracy = 86.7%; Kappa Coefficient = 75%

Source: Produced and compiled by the Researcher

Appendix 3: Mann-Kendal values for Mean Temperature and Benso, and Sefwi-Bekwai

Month	MK Test (Z)	Sen's Slope	Tau	S	Var (S)	p-Value
Benso	2.340	0.004	0.125	1694	501926	0.0169
Sefwi Bekwai	3.392	0.002	0.112	9372	7629690	0.0007

Source: Produced and compiled by the Researcher

Appendix 4: Mann-Kendal values for Mean Rainfall at Benso and Sefwi-Bekwai Stations

Meteorological Station	MK Test (Z)	Sen's Slope	Tau	S	Var (S)	p-Value
Benso	2.667	0.110	0.089	7152	7191187	0.0077
Sefwi Bekwai	0.771	0.042	0.025	2179	7970075	0.4404

Source: Produced and compiled by the Researcher